Matter

CellPress

Review

Bio-inspired anisotropic hydrogels and their applications in soft actuators and robots

Zhen Chen,[1,2] Huigang Wang,[2] Yunteng Cao,[3] Yujie Chen,[1,*] Ozan Akkus,[2] Hezhou Liu,[1] and Changyong (Chase) Cao[2,4,*]

SUMMARY

Hydrogels offer great potential for the development of soft actuators and robots owing to their water-rich structures, remarkable biocompatibility, and responsiveness to various stimuli, making them suitable for a wide range of applications. However, conventional isotropic hydrogels have limited actuation performance, hindering their functionality and practical utility. The design and synthesis of anisotropic hydrogels present a promising approach for creating high-performance soft actuators and robots. In this review, we provide an overview of the key principles involved in fabricating bio-inspired anisotropic hydrogels. We also explore the various actuation methods employed in related actuators and discuss their potential applications in soft actuators and robots. Representative research from each category is examined, highlighting the advantages and disadvantages of each approach. Furthermore, we delve into the development of intelligent hydrogel actuators and robots, showcasing their multi-functionality. Finally, we address future research challenges and provide an outlook on the field of anisotropic hydrogels.

INTRODUCTION

Organisms can adjust their shapes or motions by hydration/dehydration of cells in response to external stimuli to accommodate the changing environments.[1,2] Likewise, mollusks (such as octopuses) and inchworms can perform complex movements through muscle contraction and relaxation.[3,4] Inspired by these living organisms, researchers pay increasing attention to developing bio-inspired soft actuators and robots, aiming to enhance the integration of motile agility, extend their adaptability to unstructured environments, and achieve high work/power density. Compared to metals or elastomers, hydrogels have been extensively studied for building bio-inspired soft robotics because of their inherent softness, excellent stretchability, remarkable biocompatibility, good permeability, and responsiveness to various stimuli.[5–8]

Hydrogel-based soft actuators can generate shape morphing through the volume change induced by water transport in the hydrogel polymer network under external stimuli, such as humidity, temperature, light, pH, and magnetic and electric fields.[9–11] However, isotropic hydrogels can only generate simple deformation through volume change, which cannot meet the versatile requirements of soft actuators. Therefore, hydrogels with anisotropic structures, including those with engineered spatial patterning, have been explored to fabricate soft actuators or robots to produce more complex shape morphing, such as bending, twisting, buckling,

PROGRESS AND POTENTIAL

The design and synthesis of anisotropic hydrogels present a promising approach for creating high-performance soft actuators and robots. Here, we provide an overview of the fundamental principles involved in fabricating bio-inspired anisotropic hydrogels. We also explore the various actuation methods employed in related actuators and discuss their potential applications in soft actuators and robots. Representative research from each category is examined, highlighting the advantages and disadvantages of each approach. Furthermore, we delve into the development of intelligent hydrogel actuators and robots, showcasing their multi-functionality. Finally, we address future research challenges and provide an outlook on anisotropic hydrogels.

snapping, and 2D-to-3D shape transformation.[12] This strategy has been widely employed in nature. Many tissues have anisotropic structures across multiple hierarchical scales from the molecular to the macroscopic levels, and the built-in anisotropy in biological systems is crucial to promote efficient force generation and precise movement. For instance, skeletal muscles have an anisotropic structure formed by longitudinally aligned cylindrically shaped muscle fibers, which can generate directional contraction to drive ambulation.[13,14]

A few excellent review articles on hydrogel-based actuators have recently highlighted several aspects of this attractive material.[15,16] For example, Peng and Wang[17] summarized the shape-changing hydrogels and discussed two strategies for preparing hydrogels: inhomogeneous structures and inhomogeneous stimuli. Sano et al.[18] discussed the synthesis of anisotropic hydrogels through three methods: oriented nanofillers, polymer-chain networks, and void channels. Jiao et al.[19] reviewed the structure designs and functions of programmable morphing hydrogels under osmotic pressure actuation. However, there is a lack of comprehensive discussion on the synthesis methods, structure designs, and actuation and control methods for anisotropic hydrogels. This review will fill this gap to provide a thorough understanding of anisotropic hydrogels and their novel applications in soft robots.

The review is organized as follows. First, the development and representative strategies, including gradient/different component distributions, directional polymer-chain orientation morphology, and multi-layer structure, are described. The actuation methods for anisotropic hydrogel-based soft actuators and robots are then discussed, followed by their promising applications and models. Finally, the future research perspective and challenges for developing anisotropic hydrogels and related soft robots are presented.

FABRICATION STRATEGIES FOR ANISOTROPIC HYDROGELS

Hydrogels with anisotropic structures/components can perform shape morphing and generate anisotropic responses under external stimuli. The methods for achieving the anisotropic structures of hydrogels are mainly attributed to the anisotropic distribution of structures/components, such as additive fillers, polymer-chain networks, microfabricated structures, and macroscopic assembly. Primary design and fabrication strategies to induce anisotropy in hydrogels include gravity, electric field, magnetic field, local patterning, shear flow, polymer-chain alignment, and layered structure formation (Figure 1). This section provides an overview of the key principles and limitations of these strategies for designing anisotropic hydrogels.

Gravity-induced anisotropic hydrogels

The components of different densities in hydrogel sediment at different rates during the hydrogelation process, resulting in a gravity-induced gradient distribution of the components, such as metallic, inorganic particles, or polymer phases with different densities, thereby generating an anisotropy gradient in the structure of hydrogels. For example, Luo et al.[20] prepared a porous gradient hydrogel along the thickness direction by loading the solution containing *N*-isopropyl acrylamide (NIPAM), 4-hydroxybutyl acrylate (4HBA), and potassium persulfate into a hydrothermal reactor. In the polymerization process, NIPAM was firstly polymerized with 4HBA, forming poly(*N*-isopropyl acrylamide) (PNIPAM) chains with pendant hydroxyl groups (PNIPAM-OH). Owing to the high density of PNIPAM-OH, the concentration

[1]State Key Laboratory of Metal Matrix Composites, School of Materials Science and Engineering, Shanghai Jiao Tong University, Shanghai 200240, China

[2]Department of Mechanical and Aerospace Engineering, Case Western Reserve University, Cleveland, OH 44106, USA

[3]Department of Civil and Environmental Engineering, Massachusetts Institute of Technology, Cambridge, MA 02139, USA

[4]Advanced Platform Technology (APT) Center, Louis Stokes Cleveland VA Medical Center, Cleveland, OH 44106, USA

*Correspondence: yujiechen@sjtu.edu.cn (Y.C.), ccao@case.edu (C.C.)

https://doi.org/10.1016/j.matt.2023.08.011

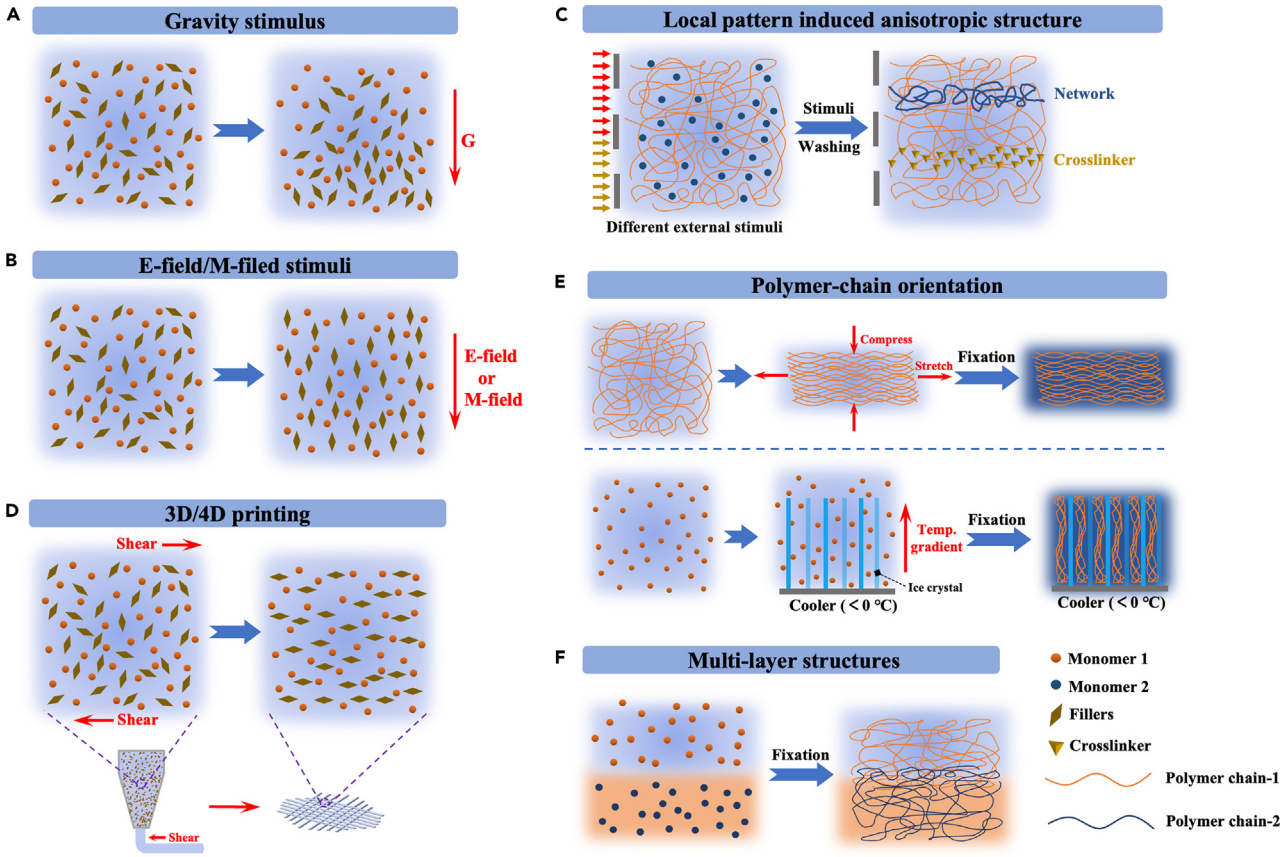

Figure 1. Schematic illustrations of anisotropic hydrogels formed with various strategies

(A) Gravity-induced anisotropy.

(B) Electric field (E-field)-induced and magnetic field (M-field)-induced anisotropy.

(C) Local-pattern-induced anisotropy.

(D) Shear-flow-induced anisotropy.

(E) Polymer-chain-alignment-induced anisotropy.

(F) Layered-structure-formed anisotropy.

gradient of PNIPAM-OH increases from top to bottom, leading to a porous gradient structure of the hydrogel (Figure 2A).

Recently, we introduced liquid metal (LM) and inorganic particles (IP) into the PNIPAM hydrogel to form a multi-directional and fast actuation hydrogel under a single stimulus.[21,22] The designed hydrogels had a gradient-distributed thermal conductivity due to the gradient distribution of fillers (LM and IP) along the thickness direction (Figures 2B and 2C). However, controlling the pore size and distribution of the hydrogel is challenging because of the competition between sedimentation and hydrogelation during the process. Additionally, the fabrication of gravity-induced anisotropic hydrogels is time consuming. Therefore, it is necessary to modify the incorporated fillers and control hydrogelation parameters precisely to adjust the gradient-distributed porous structure.

Electric-field-induced anisotropic hydrogels

The permanent or induced dipole moment in electrically charged components can be aligned along the applied electric field.[25,26] Therefore, anisotropic hydrogels can be synthesized by *in situ* hydrogelation of electrically oriented dispersions.

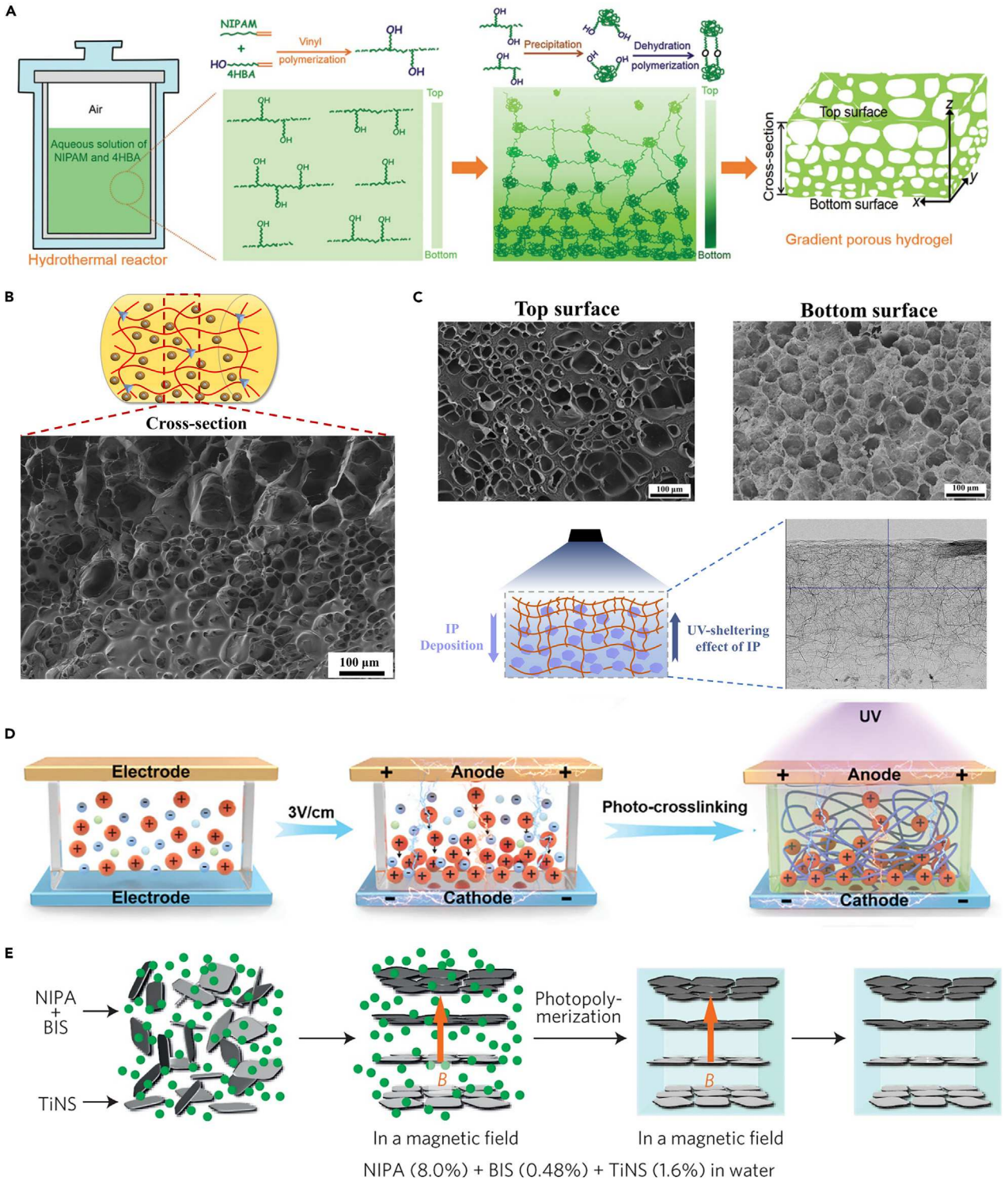

Figure 2. Anisotropic hydrogels induced by gravity, electric, and magnetic fields

(A) Polymer component was distributed with a gradient along the depth direction in the hydrogel matrix. Reprinted with permission from Luo et al.[20] Copyright 2015, Wiley-VCH.

(B) Liquid metal distributed with a vertical gradient in the hydrogel matrix. Reprinted with permission from Chen et al.[21] Copyright 2020, Elsevier.

(C) Inorganic particles distributed with a vertical gradient in the hydrogel matrix. Reprinted with permission from Chen et al.[22] Copyright 2021, Elsevier.

Figure 2. *Continued*

(D) Schematic illustration of the fabrication process for gradient-inspired gradient ionogels with electric-field induction. Under the applied electric field, the cationic crosslinkers mixed in the mold migrate toward the cathode (negative charge), resulting in a concentration gradient from the anode to the cathode. Reprinted with permission from Ren et al.[23] Copyright 2021, Wiley-VCH.

(E) Schematic illustration of the fabrication of PNIPAM-based hydrogels with co-facially oriented TiNS embedded in a magnetic field. Reprinted with permission from Kim et al.[24] Copyright 2015, Nature.

The distribution of the electrically charged components can influence the porous structure or crosslinking density of hydrogels. Ren et al.[23] proposed an electric-field-induced cationic crosslinker migration strategy to design gradient ionogels. Under an external electric field, a concentration gradient of charged crosslinkers was formed inside the mold between the cathode and the anode, followed by a hydrogelation process to stabilize the gradient structure (Figure 2D). Furthermore, multiple or micropatterned electrodes were used to program the electric-field distribution to precisely control electrically charged components in thin hydrogel sheets to form hierarchical structures.[27] For example, Xue et al.[28] developed novel near-infrared (NIR) light-driven shape-programmable hydrogel actuators with MXene. Under the DC electric field, the electrophoresis effect could achieve a gradient distribution of MXene nanosheets along the thickness of the hydrogel actuators. The photothermal effect of MXene then led to shape morphing of the hydrogel under NIR light. However, it should be noted that the applied electric fields without optimization may cause harmful electrochemical decomposition and electrophoresis during the hydrogel preparation.

Magnetic-field-induced anisotropic hydrogels

Hydrogels can generate anisotropic structures with the different distributions of magnetic particles by migrating these magnetic particles in the hydrogelation process, such as iron, Fe_3O_4, $MnFe_2O_4$, barium ferrite, carbonyl iron, nickel rods, and magnetite-coated alumina platelets.[29–34] The filler particles are aligned with their magnetization axis parallel or antiparallel to the applied magnetic field.[35] For instance, Gong et al.[36] fabricated a hydrogel with asymmetric structures by magnetic induction and subsequent *in situ* polymerization. The desired distribution of magnetic particles in the hydrogel matrix and porous structure can significantly enhance the anisotropic deformation of hydrogel-based actuators. Inspired by articular cartilage, Kim et al.[24] utilized a significant anisotropic electrostatic repulsion between negatively charged bottle brush polymers to simultaneously realize high-load-bearing and smooth mechanical joint motion and developed a hydrogel with ionic titanate nanosheets (TiNS) magnetically oriented (Figure 2E). TiNS aligned orthogonally to the applied magnetic field, generating a hydrogel with anisotropic mechanical property, i.e., the ratio of elastic moduli $E_{\perp}/E_{\parallel}$ was 3.0. The magneto-caloric effect is extensively studied for hydrogel design to produce programmable shape morphing by alternating magnetic fields (AMF).[37,38] When placed in the AMF, magnetic hydrogels can be heated due to Néel relaxation of magnetic moments to induce the phase changes of thermo-responsive polymers.[38] Besides this, the magnetic field has assisted 3D and 4D printing and biological fields thanks to its noncontact and nondestructive manner.[39–41]

The traditional magnetic-field-induced anisotropic hydrogels have limited deformation capability due to the low remanence of embedded soft magnetic particles. Recent studies proposed to utilize the magneto-thermal effect in an alternating magnetic field to actuate magnetic hydrogels.[42] However, the actuation speed is still very slow (~5 min).[38] On the contrary, some hard magnetic particles, such as neodymium iron boron (NdFeB), demonstrated high remanence and enabled programmable magnetization.[43] Nevertheless, the high density and content

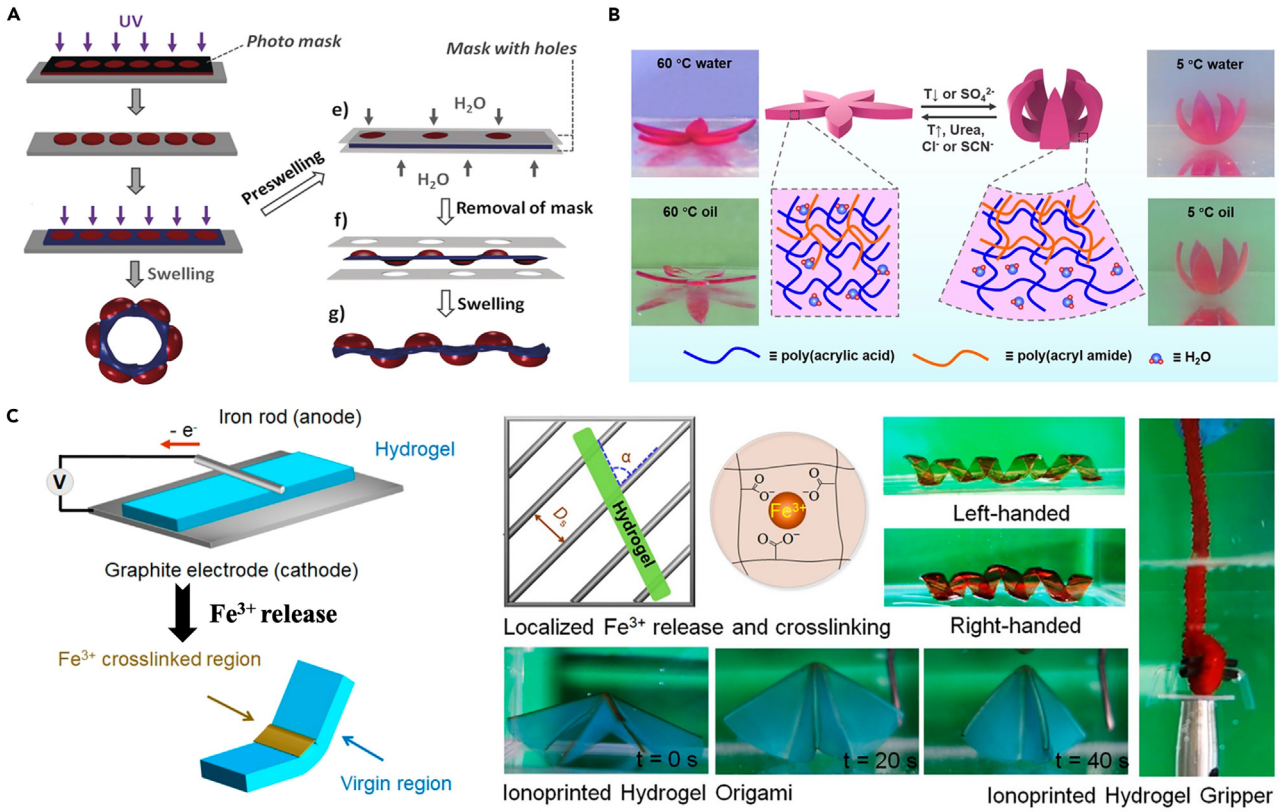

Figure 3. Local-pattern-induced anisotropic hydrogels

(A) Schematic illustration of the fabrication process of patterned hydrogels and their actuation under swelling deformations. Reprinted with permission from Wang et al.[48] Copyright 2017, Wiley-VCH.

(B) An anisotropic hydrogel formed with an asymmetric interpenetrating network can deform under temperature changes. Reprinted with permission from Hua et al.[49] Copyright 2019, American Chemical Society.

(C) Schematic illustration of releasing ferric ions into hydrogels under an electric field and the controlled 3D deformations of a hydrogel synthesized by localized Fe^{3+} release and crosslinking. Reprinted with permission from Xu and Fu.[50] Copyright 2020, American Chemical Society.

requirement to attain high remanence make these magnetic particles aggregate and settle down in the nonviscous hydrogel precursor during hydrogelation, leading to an inhomogeneous and fragile hydrogel. To solve this problem, surfactants were applied to modify the magnetic particles to retard aggregation and sedimentation, affecting magnetic responsiveness by changing the size of magnetic particles.[44] Therefore, the balance between magnetic response and structural stability of magnetic hydrogels should be considered.

Local-pattern-induced anisotropic hydrogels

Seed pods will twist into a helical structure from a flat state upon dehydration due to the variance of local compositions, and pine cones also exhibited similar anisotropic deformation.[45] Hydrogels with locally different responsive properties have gained increased attention owing to their effective actuation into complex shapes. The various responsive properties of hydrogels can be obtained by locally adjusting the compositions or structure. For example, photolithographic polymerization can produce hydrogels with macroscale/molecular-scale anisotropic structures.[46,47] Wang et al.[48] utilized the photolithographic method to introduce another hydrogel network into the as-prepared hydrogel to form an anisotropic structure, resulting in locally dissimilar swelling properties under external stimuli (Figure 3A). Similarly, through photopolymerization, Hua et al.[49] fabricated a bilayer hydrogel with a

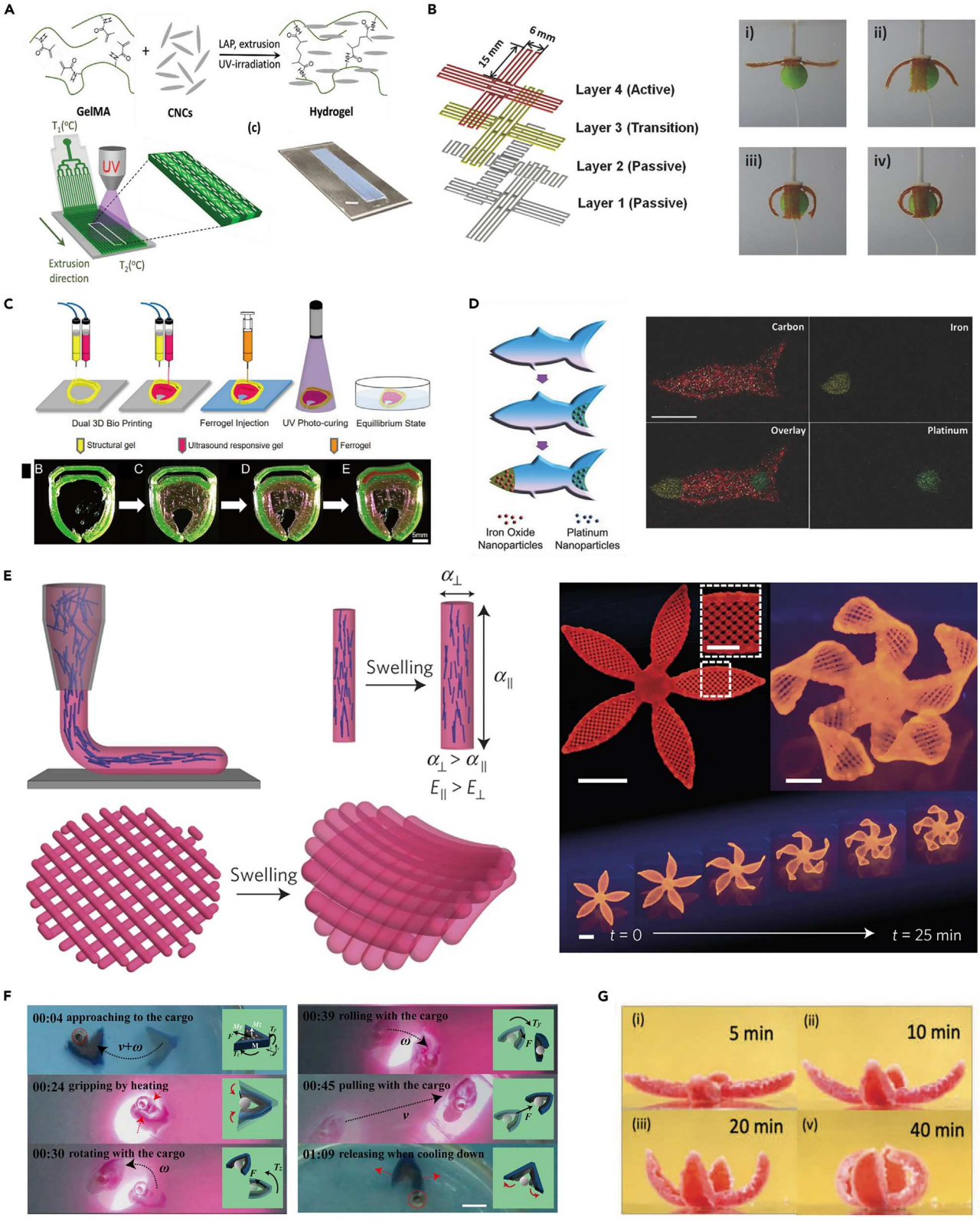
A
GelMA
CNCs
LAP, extrusion
UV-irradiation
Hydrogel
(c)
UV
Extrusion direction
B
15 mm
6 mm
Layer 4 (Active)
Layer 3 (Transition)
Layer 2 (Passive)
Layer 1 (Passive)
i)
ii)
iii)
iv)
C
Dual 3D Bio Printing
Ferrogel Injection
UV Photo-curing
Equillibrium State
Structural gel
Ultrasound responsive gel
Ferrogel
B
C
D
E
5mm
D
Iron Oxide Nanoparticles
Platinum Nanoparticles
Carbon
Iron
Overlay
Platinum
E
Swelling
Swelling
F
00:04 approaching to the cargo
00:24 gripping by heating
00:30 rotating with the cargo
00:39 rolling with the cargo
00:45 pulling with the cargo
01:09 releasing when cooling down
G
(i)
5 min
(ii)
10 min
(iii)
20 min
(v)
40 min
t = 0
t = 25 min

Figure 4. Shear flow-induced anisotropic hydrogels

(A) Anisotropic hydrogels prepared by extrusion-based 3D printing of nanocolloidal CNC/GelMa ink. Scale bar, 10 mm. Reprinted with permission from Gevorkian et al.[59] Copyright 2021, Wiley-VCH.

(B) 3D printing of anisotropic tough hydrogels to fabricate a four-finger gripper for grasping actuation. Reprinted with permission from Zheng et al.[60] Copyright 2018, Wiley-VCH.

(C) Schematic illustration of the fabrication process of a 3D-printed gripper. The nonresponsive hydrogel, ultrasound-responsive hydrogel, and magnetic-responsive ferrogel were printed sequentially. Reprinted with permission from Son et al.[61] Copyright 2020, American Chemical Society.

(D) Schematic illustration of functionalizing a microfish whereby platinum nanoparticles were loaded into the fishtail for propulsion, and iron oxide nanoparticles were loaded into the fish head for magnetic control. Scale bar, 50 μm. Reprinted with permission from Zhu et al.[62] Copyright 2015, Wiley-VCH.

(E) Shear-induced alignment of the fillers in the extrusion printing leads to the anisotropy of hydrogel. The printed petals can change their shape after swelling. Scale bar, 5 mm; inset = 2.5 mm. Reprinted with permission from Gladman et al.[63] Copyright 2016, Nature.

(F) Demonstrations of a 3D-printed shellfish-like gripper for cargo delivery and a *Leptasterias*-like gripper for active delivery in a stomach model. Scale bar, 6 mm. Reprinted with permission from Hu et al.[64] Copyright 2022, Elsevier.

(G) Shape transition of a 3D-printed hydrogel flower wraps up from a flat state to a 3D blooming state after being immersed in water (50°C). Reprinted with permission from Shiblee et al.[65] Copyright 2019, Wiley-VCH.

single-network structure in the bottom layer and a double network in the top layer due to poor UV light penetration. Distinct volume changes of the various layers under the thermal stimuli led to anisotropic deformation (Figure 3B). On the other hand, Kim et al.[51] used the photolithographic method to locally change the crosslinking densities of PNIPAM hydrogels by controlling the local irradiation dose. The different parts of the obtained hydrogels underwent various shape changes under external thermal stimuli, enabling complex shape changes such as saddles, domes, and plates with waved edges. Moreover, adjusting light-exposure time related to crosslinking density can provide the patterned anisotropic structure.

The crosslinking density change of ferric ions and the carboxyl groups of hydrogels based on the reduction reaction from Fe^{3+} to Fe^{2+} under UV light or acid have been employed in designing actuating hydrogels.[52,53] Introducing metal ions into hydrogel systems through electrochemical ionoprinting, ion-transfer printing, or ion-inkjet printing are also reported as effective methods.[54,55] With the help of an electric field, Xu and Fu[50] reported a programmable and reversible shape-morphing hydrogel by precise infiltration of Fe^{3+} with periodic patterns to form the local crosslinking network by ionoprinting with a patterned electrode array (Figure 3C). The local crosslinking created slight undulations of local stresses and responsive properties in hydrogel sheets. Thus, it underwent 3D shape deformations to form helices with predictable and tunable chirality, spacing, and tilting angles.

Shear-flow-induced anisotropic hydrogels

3D/4D printing is a novel additive manufacturing technique to fabricate anisotropic hydrogels with micro-/macrostructures. During the 3D-printing process, hydrogel precursor inks containing high-aspect-ratio fillers, such as nanoclay, metal nanorods, carbon nanotubes (CNTs), cellulose nanofibers, and cellulose nanocrystals (CNCs), can be well aligned by the shear forces generated in the extrusion process to form anisotropic structures in the 3D-printed hydrogel.[56–58] For example, Gevorkian et al.[59] developed a 3D-printed actuator with nanocolloidal hydrogels made of rod-like CNCs and methacryloyl gelatin (GelMa). The shear-induced uniaxial orientation of CNCs enabled the anisotropic structure that can generate complex and programmable stimulus-responsive shape transitions (Figure 4A). The hydrogel sheet can be programmed by adjusting the degree of orientation of CNCs and the configurations of responsive and nonresponsive regions.

In addition to the shear-induced alignment of high-aspect-ratio particles, the responses of hydrogels can be designed by controlling the hydrogel composition. For example, Zheng et al.[60] employed a 3D printer with multiple nozzles to integrate

both responsive and nonresponsive gel fibers into a single hydrogel actuator. The alignment of responsive gel fiber enabled controlled deformations under external stimuli (Figure 4B). Similarly, Son et al.[61] utilized a dual-material 3D printer to fabricate hybrid hydrogel grippers (Figure 4C). In their design, the exterior layer of the gripper was printed with nonresponsive acrylamide (AM)-based gel, while the interior layer was printed with NIPAM-based gel, which is responsive to ultrasound actuation. AM-based ferrogel was further injected into the wells to form hybrid hydrogel under UV polymerization. The 3D-printed hybrid actuators can perform simultaneous locomotion and actuation control through external magnetic fields and low-intensity ultrasound.

In addition, 3D printing can be combined with other fabrication techniques, such as photolithography and hydrogel electrospinning, to create mixed-mode fabrication platforms.[66] For example, Zhu et al.[62] fabricated a microrobotic fish with 3D printing of multiple types of functional nanoparticles in the tail and head part, respectively, to precisely control the motion of the fish, whose hydrogel body was fabricated via UV photolithography (Figure 4D). Agarwal et al.[67] combined 3D printing with electrospinning to manufacture temperature-responsive actuators. The electrospun mesoporous substrate provided rapid responses due to the fast mass transfer of the porous structure. The rigid pattern was 3D printed on the substrate to provide a template to induce 3D deformations.

The new concept of 4D printing refers to 3D-printed structures that transform over time in response to environmental stimuli.[40,63,68,69] In this regard, Gladman et al.[63] proposed a 4D-printed biomimetic hydrogel with localized swelling anisotropy. The programmable hydrogel structures patterned in space and time can achieve complex deformation on immersion in water (Figure 4E). Hu et al.[64] fabricated a smart nanocomposite hydrogel that can respond to magnetic field and temperature via the 4D-printing technique. A double-layer film was fabricated as the actuation unit to realize bending deformation under a thermal field. Furthermore, dual-responsive hydrogel robots were fabricated using 4D printing for cargo and drug delivery (Figure 4F). Shiblee et al.[65] integrated 4D-printing technology with shape-memory hydrogels (SMHs) to develop a mechanically robust, soft bilayer actuator using two active layers. They designed a 4-petal flower that can deform from a flat shape to a 3D closing state by swelling and an underwater soft gripper that can perform accurate gripping, transportation, and release of a glass vial upon swelling in water (Figure 4G).

Polymer-chain alignment for anisotropic hydrogels

The oriented fiber structure is essential for animals or plants in nature to achieve their different functions or activities.[19] Inspired by such bio-structures, introducing a polymer-chain-oriented structure into the hydrogel system has been used to improve its performance and functionality. Current methods mainly include the ice-template method and unidirectional strain assistance.

Ice template (or freeze-casting) is a promising method for advanced materials design and fabrication, due to its attractive merits of precise architecture control, easy scalability, versatility, and low cost.[70–72] When an aqueous monomer solution in a container is immersed slowly in a freezing medium (e.g., liquid nitrogen), ice crystals will grow unidirectionally from the immersed bottom, which has higher heat conductivity. With the ice crystals serving as templates, an anisotropic structure will form during hydrogelation, leading to polymer chains aligned with the freezing direction in the hydrogel. Zhao et al.[73] developed an unconventional one-pot synthesis

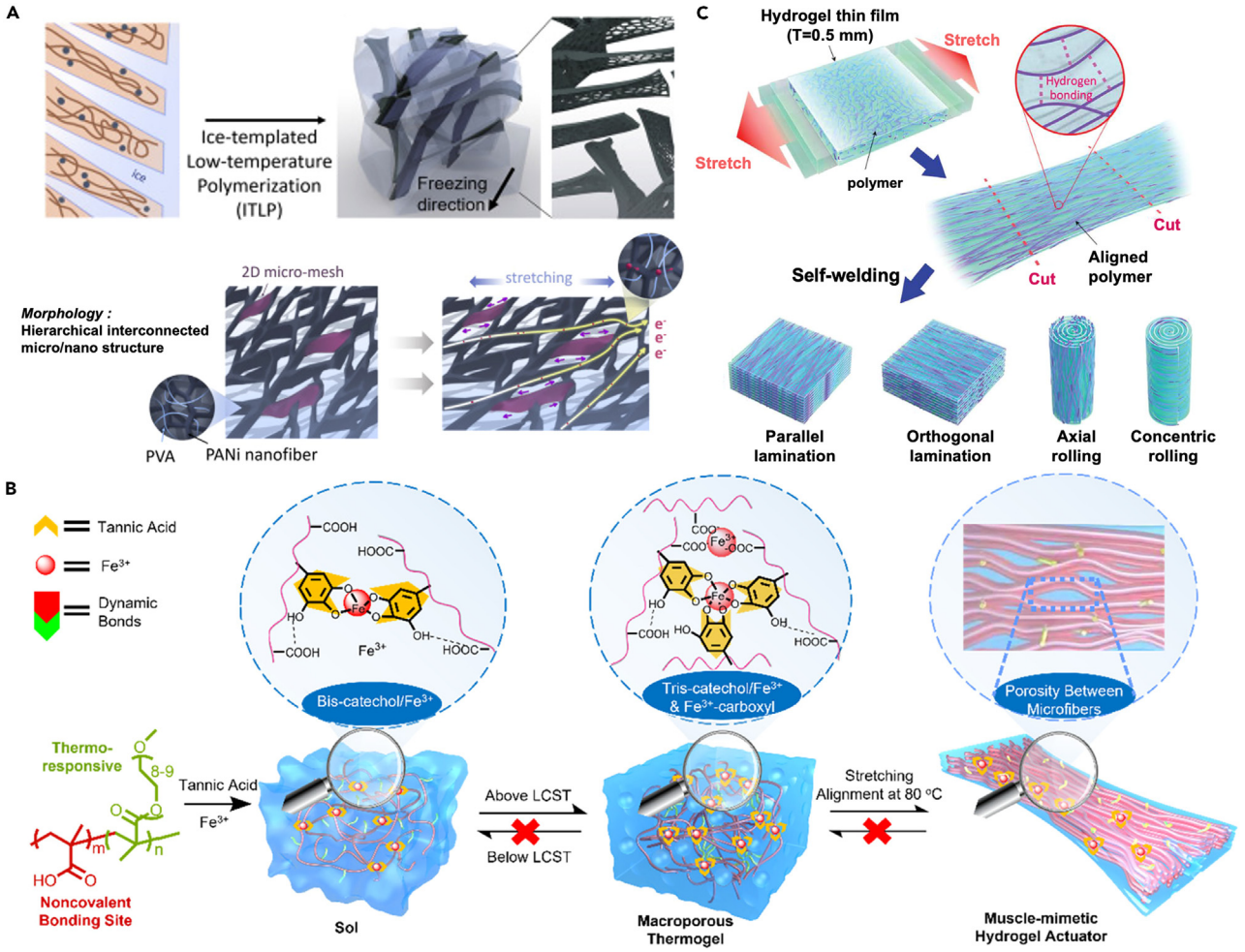

Figure 5. Ice template and strain-induced polymer-chain orientation for anisotropic hydrogels

(A) Schematic illustration of the aligned dendrite microstructure formed with the ice template and the hierarchical interconnected micro-/nanostructure benefiting from the electrical conduction in the hydrogel by ice-templated low-temperature polymerization. Reprinted with permission from Zhao et al.[73] Copyright 2021, Science.

(B) Schematic illustration of a hydrogel actuator fabricated by a combination of thermo-induced phase separation and mechanical alignment. Reprinted with permission from Jiang et al.[74] Copyright 2021, American Chemical Society.

(C) Schematic illustration of weldable multilayered anisotropic cellulose hydrogels and self-welding process of hydrogel layers with the assistance of stretching. Reprinted with permission from Mredha et al.[75] Copyright 2019, Royal Society of Chemistry.

method to design the single monolithic hydrogel for sensory actuation via the ice-template approach. The precursor mixture of PNIPAM and polyaniline (PANI) was rapidly frozen in liquid nitrogen (−196°C) to form an ice template, followed by UV- and cryo-polymerization of PNIPAM and PANI in a subzero environment (−20°C). The resulting hydrogel exhibited higher mechanical properties with a 29-fold enhancement in toughness along the freezing direction (Figure 5A). Moreover, the hydrogel had continuous pathways for electron conduction. It demonstrated an 83-fold increase in conductivity due to the suppressed PANI-nano-aggregate overgrowth under subzero reaction and the densified PANI packing by ice templating. They recently proposed a strong and tough poly(vinyl alcohol) (PVA) hydrogel using the synergy of ice template and salting-out effect. The PVA hydrogels were highly anisotropic and had micrometer-scale honeycomb-like pore

walls and interconnected nanofibril meshes, resulting in high strength, toughness, stretchability, and fatigue resistance.[76]

Besides this, when isotropic hydrogels are stretched or compressed uniaxially, their network will deform with the polymer-chain alignment. The induced temporal anisotropy can be fixed by physical or chemical interactions (e.g., *in situ* hydrogelation, hydrophobic association, ionic coordination, host-guest inclusion, hydrogen bonding) to form anisotropic hydrogels.[77–80] These interactions can be reversibly eliminated or dissociated under proper stimuli to recover hydrogels to their initial state.[81] Li et al.[82] proposed the photo-dissociable Fe^{3+}-carboxylate coordination as a molecular switch to realize the photocontrol of shape memory on macroscopic and microscopic scales. They chose sodium alginate (SA)/polyacrylamide (PAM) hydrogel, bearing carboxylate groups that bind with Fe^{3+} and other multivalent ions, as a model material. After the hydrogelation, the hydrogel can be stretched to different 2D patterns and then immersed into aqueous solutions containing Fe^{3+} ions to form Fe^{3+}-carboxylate coordination for strain fixation, while light irradiation through phototriggered reduction of Fe^{3+} to Fe^{2+} led to strain relaxation and shape recovery. However, one drawback of the metal-ligand coordination hydrogel is its slow shape deformation. A large amount of water molecules in the network also facilitates chain motion, thus weakening the fixation of deformation.

To improve the compatibility between actuation speed and mechanical properties, Jiang et al.[74] reported a new concept to fabricate hydrogel actuators with a muscle-like aligned microfibrillar architecture based on a combination of thermo-induced phase separation and mechanical alignment. A thermo-responsive polymer was physically engineered with metal-phenolic complexes at the molecular level to generate macroporous thermo-gels with bundled networks via irreversible thermal sol-gel transition. A muscle-like oriented microfibrillar architecture was then obtained by stretching alignment at an elevated temperature via a network rearrangement, resulting in a high degree of porosity due to the gap between microfibers, resulting in ultrafast reversible thermo-actuation (<1 s) (Figure 5B). This result demonstrated that aligned microfibrillar morphology could improve shape-changing speed and mechanical properties simultaneously. Therefore, the unidirectional freeze-casting technique and strain assistance both modulated conventional hydrogel materials with aligned micro-/nanostructures, resulting in superior fatigue resistance along the alignment direction. However, the fatigue threshold perpendicular to the alignment is still limited. Inspired by the distinct structure-property relationship of heart valves, Wei et al.[83] employed a bidirectional ice-template process and compression annealing to form a 2D isotropic fatigue-resistant hydrogel with aligned lamellar micro-/nanostructures. The final hydrogel exhibited unprecedented fatigue thresholds of over 1,500 J m^{-2} along any in-plane direction, superior to most reported hydrogel systems.

In addition, Mredha et al.[75] proposed a novel welding technique to fabricate anisotropic tough multi-layer hydrogels with differently oriented hierarchies: parallel lamination, orthogonal lamination, axial rolling, and concentric rolling (Figure 5C). They applied cellulose/dimethylacetamide/lithium chloride solution to melt the contact parts (welding area) of stretched cellulose hydrogel films. The ion-induced interfacial reconfiguration of polymer chains enabled bonding at the welding area. Although the final hydrogel had high water content (~68 wt %), it exhibited extremely high optical anisotropy (birefringence $\geq$0.006) and elevated mechanical properties (Young's modulus of ~140 MPa, tensile strength of ~47 MPa, and work of extension of ~20 MJ m^{-3}).

Layered-structure-formed anisotropic hydrogels

Multi-layer hydrogels can achieve bulk heterogeneity by combining the isotropic or anisotropic single layers with different responsive properties. As one of the simplest models, bilayer hydrogels are usually prepared by layer-by-layer polymerization. The bonding between layers is essential to the functionality and durability of the hydrogel devices, which are generally related to the interlocking interfaces between the hydrogels, such as interpenetrating polymer networks, electrostatic interactions, or host-gust interactions.[84–89] We recently reported a bilayer hydrogel formed by PNIPAM and poly(acrylamide-acrylic acid) (P(AM-AA)) hydrogels via an interpenetrating polymer at the interface acting as a junction to connect the two layers (Figure 6A).[90] For electrostatic interaction, polyanion or polycation is generally involved in the design of hydrogel layers. Mredha et al.[75] used electrophoresis to deliver polyions into the gels and formed a polyion complex at the interface of the two gels for adhesion. During this process, two PNIPAM gels with linear chains, consisting of a polyanion or polycation, showed outstanding adhesion to one another upon electric-field impression and formed entangled polymer networks. Additionally, Ma et al.[91] synthesized the bilayer actuation hydrogel with tunable fluorescence by combining a thermo-responsive graphene oxide-poly(*N*-isopropylacrylamide) (GO-PNIPAM) hydrogel layer with a pH-responsive perylene bisimide-functionalized hyperbranched polyethyleneimine (PBI-HPEI) hydrogel layer. A designed supramolecular glue (poly(acrylamide-co-*N*-adamantyl acrylamide)) was applied to tightly bond two layers based on host-guest interaction (Figure 6B).

The aforementioned noncovalent interface interactions are usually weak and suffer from interface instability after long-term applications. Therefore, several methods, such as covalent bonding and mechanical interlocking between layers, have been proposed to improve the stability of multi-layer hydrogels. Li et al.[93] designed an asymmetric bilayer CNTs-elastomer/hydrogel composite with actuation and sensing. In this work, covalent bonding was applied to achieve material adhesion with different characteristics. The prepared CNTs-elastomer film was immersed into an ethanol solution containing the photoresponsive initiator benzophenone to allow the diffusion of benzophenone into the film. The polymerization of NIPAM was then initiated on the Ecoflex surface to obtain a CNTs-Ecoflex/PNIPAm hydrogel composite. Recently, mechanical interlocking between layers has been considered to enhance layer connection. Hubbard et al.[92] proposed trilayer hydrogel-elastomer laminates bonded via glass fiber (GF) fabric interphases to achieve stimulus-responsive actuation. The hydrogel-elastomer laminates were produced via a two-step fabrication, resulting in the GF fabric being physically trapped between polydimethylsiloxane (PDMS) elastomer and polyampholyte (PA) hydrogel. The GF fabric interacted strongly with the soft laminated phases, and the elastomer phase was physically interlocked, permeating even the individual bundles (Figure 6C). In contrast, the hydrogel primarily interacted with the glass surface via electrostatic interactions. The adhesive structure exhibited maximum interfacial adhesion energies of $\sim$1,000 N m^{-1} between the hydrogel and fabric and $\sim$360 N m^{-1} between the elastomer and fabric, approaching the adhesion values of chemically bound soft materials.

It should be noted that the deformation rates of multi-layer hydrogels usually depend on the swelling/deswelling rates, the thicknesses, and the moduli of component layers. Thus, their shape changes can be programmed by designing the locations and shapes of the layered hydrogels or by constructing different hydrogel parts. Over the past years, hydrogel actuators with multi-layer structures have

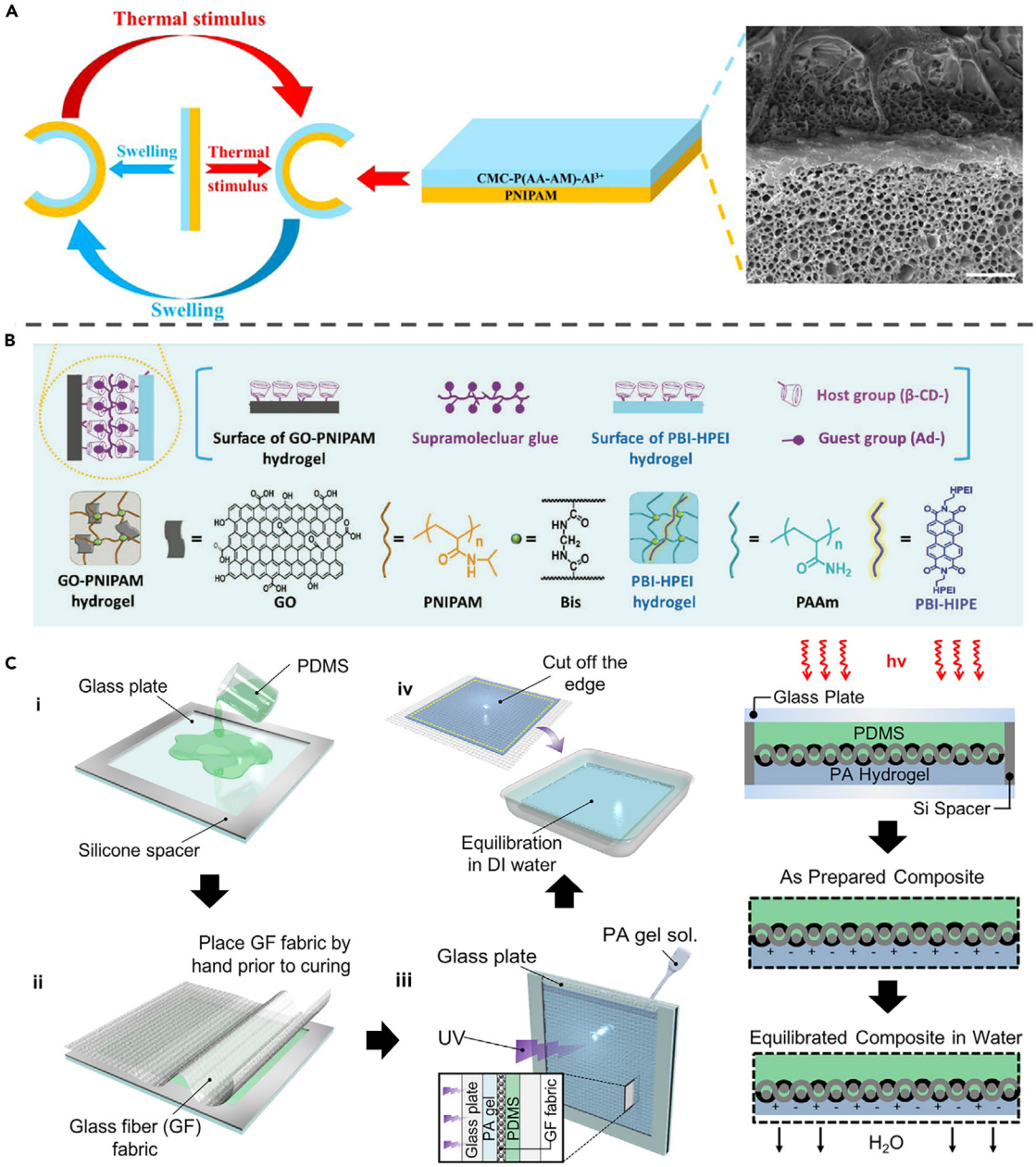

Figure 6. Multi-layer anisotropic hydrogels with different interface structure designs

(A) A bilayer hydrogel made of interpenetrating polymer networks. It can be actuated with either swelling or thermal stimulus. Scale bar, 1 cm. Reprinted with permission from Chen et al.[90] Copyright 2021, American Chemical Society.

(B) Layered anisotropic hydrogel formed by host-guest interaction at the interface. Reprinted with permission from Ma et al.[91] Copyright 2018, Wiley-VCH.

(C) Layered anisotropic hydrogel via mechanical interlocking bonding between the layers. Reprinted with permission from Hubbard et al.[92] Copyright 2019, Elsevier.

been increasingly reported. However, they could only perform limited variations of simple shape deformations. Exploring other inhomogeneous structures or configurations will be essential to expand their potential applications and enrich the diversity of deformations.

Table 1. Representative examples of hydrogel actuators with different anisotropic structure designs

Anisotropic structure design strategies	Hydrogel	Max. stress (MPa), strain	Actuation force (N)	Actuation frequency (Hz)	Stimulus-responsive cycle (service life)	Pros and cons	Reference
Gravity	BN + PNIPAM	0.018, 200%	0.1	0.008	≥10 cycles	universality and easy preparation but poor actuation force/ uncontrolled structure	Chen et al.[22]
	PNIPAM-OH	0.1, 95%	0.007	0.06	≥5 cycles		Luo et al.[20]
	PDA-LM + PNIPAM	N/A, N/A	0.03	0.025	≥10 cycles		Chen et al.[21]
Electrical field	MXene + PNIPAM	N/A, N/A	N/A	0.02	≥10 cycles	controlled structure design and easy functionality but limited actuation force	Xue et al.[28]
	PNIPAM-Au	0.015, 150%	N/A	0.1	≥5 cycles		Zhu et al.[94]
	PAA-PAM-Cu	N/A, N/A	0.005	0.01	≥10 cycles		Palleau et al.[54]
Magnetic field	P(NaAMPS-AM)	1.6, 1600%	N/A	1.0	N/A	controlled structure design and function but magnetic-field-intensity-dependent actuation	Tang et al.[41]
	Fe_3O_4@TCNCs + P(AA-AM)	N/A	N/A	0.001	≥10 cycles		Gong et al.[36]
	alginate-Fe_3O_4	55, 80%	0.1	10	N/A		Zhao et al.[95]
Local pattern	P(AA-AM)-PAA	N/A	N/A	0.007	≥10 cycles	controlled structure design and diverse response but limited mechanical properties	Hua et al.[49]
	P(NIPAM-NaMAc) + Fe^{3+}	0.16, 50%	0.005	0.02	≥5 cycles		Xu and Fu[50]
	GO-PNIPAM	N/A	0.004	0.02	≥5 cycles		Ma et al.[96]
Shear flow	P(AA-AM) + P(AA-NIPAM)	2.5, 800%	0.15	0.02	≥10 cycles	controlled and diverse structure design but complex preparation	Zheng et al.[60]
	PAA-Zr^{4+}	1.3, 800%	0.49	N/A	N/A		Dong et al.[97]
Ice template	PANI-PNIPAM	0.016, 75%	0.055	0.03	N/A	good mechanical properties and actuation force but complicated design and poor function	Zhao et al.[73]
	PVA-GO	9, 250%	50.24	0.03	≥30,000 cycles		Liang et al.[83]
Strain induction	P(AM-AA)-Fe^{3+}	3.7, 600%	0.45	0.0003	≥5 cycles	good mechanical properties and actuation force but complicated design	Ma et al.[98]
	P(MEO_2MA-OEGMA-NIPAM)	3, 320%	N/A	0.006	≥20 cycles		Wei et al.[81]
	P(MAA-OEGMA)	1.3, 300%	0.025	0.1	≥10 cycles		Jiang et al.[74]
Multi-layer	CNTs-Ecoflex + PNIPAM	N/A	N/A	0.07	≥10 cycles	easy functionality and preparation but limited stability	Li et al.[93]
	CMC-P(AA-AM) + PNIPAM	0.339, 980%	0.143	0.007	≥10 cycles		Chen et al.[90]

BN, boron nitride; GO, graphene oxide; PNIPAM, poly(*N*-isopropyl acrylamide); PDA, polydopamine; EGaIn, eutectic indium gallium; PAM, polyacrylamide; PAA, polyacrylic acid; PAMPS, poly(2-acrylamide-2-methylpropanesulfonic acid); PANI, polyaniline; P(MEO_2MA-OEGMA-NIPAM), poly (2-(2-methoxyethoxy) ethyl methacrylate-co-oligo-(ethylene glycol) methacrylate-co-isopropylacrylamide; Zr, zirconium; P(MAA-OEGMA), poly(methacrylic acid-co-oligo(ethylene glycol) methacrylate; TA, tannic acid; CNT, carbon nanotube; CMC, sodium carboxymethylcellulose; N/A, specific value not provided.

In summary, to meet various property requirements, different anisotropic structures have been developed to suit different application scenarios. To provide clarity, a comprehensive comparison of different anisotropic structure strategies has been compiled in Table 1.[20–22,28,36,41,49,50,54,60,73,74,81,83,90,93–98] This comparison encompasses mechanical properties, actuation force, actuation frequency, and life cycle, as well as the advantages and disadvantages of each strategy. In addition, we have compiled and compared the frequently investigated polymer backbones used in various anisotropic structure design strategies for hydrogels (Table 2).[20–22,27,28,36,39,41,48,49,54,71,82,83,90,91,93,94,98–102] We anticipate that these comparisons will offer researchers a direct and comprehensive understanding of the diverse approaches in anisotropic structure design for hydrogels.

ACTUATION METHODS FOR ANISOTROPIC HYDROGEL-BASED SOFT ACTUATORS AND ROBOTS

Effective and efficient actuation and control are critical for anisotropic hydrogel-based actuators and robots to achieve their full potential in various applications. There are two major categories of actuation: active and passive (Table 3).[21,22,41,54,60,63,95,98,103–108]

Table 2. Representative polymer backbones, corresponding functions, polymerization methods, and pros and cons for different anisotropic structure designs

Anisotropic structure strategies	Commonly used polymer backbone	Polymer functions	Polymerization methods	Pros and cons	References
Gravity	PNIPAM	thermal response	UV/thermo-induced polymerization	easy polymerization but poor mechanical properties	Luo et al.,[20] Chen et al.,[21] Liu et al.[99]
	PNIPAM-OH	thermal response	thermo-induction polymerization	easy polymerization/ modification but poor mechanical properties	Chen et al.[22]
Electrical field	polyelectrolyte	electrical response	physical crosslinking	good mechanical properties but poor solubility/functions	Yang et al.[27]
	PNIPAM	supporting matrix/ photothermal conversion	UV-induced polymerization	easy functionality but poor mechanical properties	Xue et al.,[28] Zhu et al.[94]
Magnetic field	PAA/PAMPS + PAM	supporting matrix	UV-induced polymerization	suitable mechanical properties and easy polymerization but limited functions	Gong et al.,[36] Tang et al.[41]
	PNIPAM	supporting matrix/ magnetocaloric effect	thermo-induced polymerization	easy functionality but poor mechanical properties	Tang et al.[39]
Local pattern	PAA/PAMPS + PAM	functional matrix	UV-induced polymerization	easy polymerization but limited functions	Wang et al.,[48] Hua et al.,[49] Palleau et al.[54]
3D printing	alginate-PAM + Ca^{2+}	supporting matrix	UV-induced polymerization	easy polymerization/suitable mechanical properties but poor functions	Park and Kim,[100] et al.[101]
	PEGDA	supporting matrix	UV-induced polymerization	easy polymerization but poor printing resolution	Arslan et al.[102]
Ice template	PVA	supporting matrix/ freezing crystallization	UV-induced polymerization	good mechanical properties but poor modification	Feng et al.,[71] Liang et al.[83]
Strain induction	PAA/PAM + Fe^{3+}	functional matrix	UV-induced polymerization	good mechanical properties but limited functions	Li et al.,[82] Ma et al.[98]
Multi-layer	PAA/PAM/ PNIPAM	functional matrix	UV/thermo-induced polymerization	easy polymerization but limited performance	Chen et al.,[90] Ma et al.,[91] Li et al.[93]

PNIPAM, poly (*N*-isopropyl acrylamide); PAMPS, poly (2-acrylamide-2-methylpropanesulfonic acid); PEGDA, poly (ethylene glycol diacrylate); PVA, polyvinyl alcohol.

Active actuation, including osmotic pressure and elastic potential energy actuation, refers to hydrogels actively performing the molecular or structural change under external stimuli. Passive actuation relates to responsive particle actuation and pneumatic/hydraulic actuation, whereby hydrogels serve as carriers to confront external stimuli and perform the deformation passively through the active actuation sources, such as pneumatic/hydraulic pressure or responsive particles.

Osmotic pressure actuation

The osmotic pressure actuation of hydrogel actuators has been extensively researched. It relies on the swelling and deswelling behaviors of hydrogels under external stimuli, such as solvent, temperature, electric field, pH, temperature, salts, light, and molecules.[109–111] The osmotic pressure changes of hydrogels and surrounding environments result in water diffusion in and out of the hydrogels, thereby generating expansion and contraction for actuation. Therefore, the osmotic pressure depends on the concentrations of water, charged ions or groups, and different interactions between polymer, water, and environments.[112] Further, the osmotic pressure of hydrogels can be measured by two methods, one of which is the employment of semi-permeable membranes.[113,114] However, the limited membrane strength makes it only suitable for the osmotic pressure of hydrogels with low polymer concentrations or low osmotic pressure inside it. In addition, the osmotic pressure can be calculated based on the equations of states of hydrogels with

Table 3. Representative examples of hydrogel actuators with different actuation and control methods

Actuation and control methods		Hydrogels	Max. stress (MPa), strain (%)	Stimuli	Actuation force (N)	Actuation frequency (Hz)	References
Active actuation	osmotic pressure actuation	NFC + PDMAM	0.05, 320%	water	0.001	0.001	Gladman et al.[63]
		BN + PNIPAM	0.018, 200%	temperature	0.10	0.008	Chen et al.[22]
		PDA-LM + PNIPAM	N/A, N/A	temperature	0.03	0.025	Chen et al.[21]
		PAM + αCD + Azo	0.091, 220%	light	0.001	0.002	Takashima et al.[103]
		P(AA-AM) + P(AA-NIPAM)	2.5, 800%	saline solution	0.15	0.02	Zheng et al.[60]
		PAA + PAM + Cu	N/A, N/A	electric field	0.005	0.01	Palleau et al.[54]
	elastic potential energy actuation	P(AM-AA)-Fe^{3+}	3.7, 600%	ions	0.45	0.0003	Ma et al.[98]
		PAA/Ca $(CH_3COO)_2$	0.2, 315%	ions	0.182	0.001	Hua et al.[104]
Passive actuation	responsive particle actuation	PAM-NaCl	N/A, 50%	electric field	0.005	100	Keplinger et al.[105]
		PAM-LiCl	N/A, N/A	electric field	0.007	10	Li et al.[106]
		alginate-Fe_3O_4	0.055, 80%	magnetic field	0.1	10	Zhao et al.[95]
		PAM-PNaAMPS-NdFeB	1.6, 1800%	magnetic field	N/A	1.0	Tang et al.[41]
	pneumatic & hydraulic actuation	gelatin-alginate-Ca^{2+}	0.75, 75%	pneumatic pressure	N/A	0.1	Wu et al.[107]
		PAM-alginate	0.035, 300%	hydraulic pressure	1.0	2.0	Yuk et al.[108]

NFC, nanofibrillated cellulose; PDMAM, poly(*N*,*N*-dimethylacrylamide); PNIPAM, poly(*N*-isopropyl acrylamide); BN, boron nitride; PDA, polydopamine; EGaIn, eutectic indium gallium; CD, cyclodextrin; Azo, azobenzene; PAA, polyacrylic acid; PAM, polyacrylamide; Cu, copper; NaCl, sodium chloride; LiCl, lithium chloride; Fe_3O_4, iron oxide; PNaAMPS, poly(2-acrylamido-2-methyl-1-propanesulfonic acid sodium salt); NdFeB, Magnequench MQFP-B-20076-089; N/A, specific value not provided.

different deformations, such as volume conservation and free energy conservation.[115,116] In recent reports from the literature, osmotic pressure actuation of hydrogels usually suffers from low response speed (minutes to hours) due to the osmotic swelling proceeding with the low diffusion of water in hydrogel matrices. Therefore, high water diffusion or porosity structure is essential to improve the actuation speed of this actuation mechanism. Many approaches for hydrogel fabrication have been proposed to improve actuation speed, including incorporating thermal fillers, porogens, the molecular engineering of stimuli-responsive hydrogels, freeze-thaw, co-nonsolvency photopolymerization, hydrothermal process, and electro-osmosis (Table 4).[20–22,74,99,117–123] For example, Jian et al.[124] utilized ice as the porogen to construct PNIPAM hydrogels with large pores. During the low-temperature polymerization, monomers were confined and polymerized to form the local polymer networks owing to the presence of ice crystals. The ice crystals melted with increasing temperature, and larger micropores filled with water were obtained (Figure 7A). The final hydrogel sponge exhibited fast swelling/deswelling capacity (equilibrium time 7 s) compared with the ordinary PNIPAM hydrogels (deswelling >1 min, swelling >20 min). However, a hydrogel with overly high porosity usually lacks the rigidity for practical applications. Simultaneously enhancing diffusion and mechanical properties remains a long-standing challenge. To balance the high porosity and suitable mechanical properties, Alsaid et al.[118] proposed a novel approach to overcome this swelling-mechanical property trade-off by using co-nonsolvency photopolymerization, in which PNIPAM was polymerized in DMSO/water cosolvent mixtures. In the hydrogelation, simultaneous crosslinking and co-nonsolvency-induced polymer collapse resulted in hierarchically structured and interconnected polymer networks. The designed hydrogel exhibited 2-fold enhancements in swelling ratio and Young's modulus and a 6-fold enhancement of deswelling rate compared to the hydrogel synthesized with a conventional pure solvent method. Na et al.[119] employed electro-osmosis to improve the swelling of hydrogels, whereby the migrating ions drag the adjacent water into the charged polymer network under an electric field. In addition, the diffusion rate of water in the osmotic

Table 4. Representative examples of osmotic-pressure-based hydrogel actuators with enhanced response speeds

Methods	Hydrogels	Structures	Pros and cons	References
Molecular engineering	PMAA-POEGMA/Fe^{3+}	aligned microfibrillar	high performance improvement but complicated design/ preparation	Jiang et al.[74]
	rGO/PDMAEMA	dual-gradient structures		Fan et al.[117]
Co-nonsolvency photopolymerization	PNIPAM	sponge-like mesoporosity	high performance improvement but limited hydrogel systems	Alsaid et al.[118]
Electro-osmotic turgor pressure	polyelectrolyte gel/ membrane	gel confined by a selectively permeable membrane	high performance improvement but complicated structure design	Na et al.[119]
Adding of thermal fillers	PDA + EGaIn-PNIPAM	gradient distribution of EGaIn and pore	universality and easy preparation but uncontrolled structure/filler-dependent performance	Chen et al.[21]
	BN/ALN/Si_3N_4-PNIPAM	gradient distribution of BN/ALN/Si_3N_4 and pore		Chen et al.[22]
	MMT	gradient distribution of MMT and pore		Liu et al.[99]
Porogen	PNIPAM/PAA/PAM-PEG	bilayer structure with porosity	universality and easy preparation but limited performance improvement	Zheng et al.[120]
Freeze-thaw	PVA/PANI	porous structure	universality and easy preparation but limited performance improvement	Li et al.[121]
	PASH	porous structure		Chen et al.[122]
	PMAA-POEGMA	porous structure		Jiang et al.[123]
Hydrothermal process	PNIPAM-OH/PPy	gradient porous structure	universality but limited performance improvement/uncontrolled structure	Luo et al.[20]

PMAA, polymethylacrylic acid; POEGMA, poly oligo(ethylene glycol) methacrylate; rGO, reduced graphene oxide; PDMAEMA, poly(*N*,*N*-dimethylaminoethyl methacrylate); ALN, aluminum nitride; Si_3N_4, silicon nitride; MMT, montmorillonoid; PEG, polyethylene glycol; PVA, polyvinyl alcohol; PANI, polyaniline; PASH, polyaniline/poly(acrylamide-sodium acrylate); PPy, polypyrrole.

pressure actuating hydrogel is inversely proportional to the square of its dimension.[108]

Yuk et al.[108] proposed an osmotic pressure actuation force F evaluation and the responsive time t scale as

$$F \propto \Delta\Pi L^2, t \propto L^2/D, \quad \text{(Equation 1)}$$

where $\Delta\Pi$, D, and L are the osmotic pressure change, the diffusivity of water in the hydrogel, and a typical dimension of the block, respectively. In the case of osmotic pressure actuation, there exists an inherent trade-off between actuation force and response time. Larger deformations in hydrogels correspond to higher actuation forces but result in longer response times. As a consequence, the actuation force and response time tend to be incompatible in osmotic pressure-actuated hydrogel actuators.[24,125,126] Achieving a balance between actuation force and actuation speed remains an open area of investigation for stimuli-responsive hydrogels actuated by osmotic pressure. Addressing this challenge is crucial to optimize the performance and applicability of such hydrogel-based actuators.

Elastic potential energy actuation

Elastic potential energy actuation widely exists in animals, especially when jumping.[127–129] Unlike osmotic pressure actuation, elastic potential energy actuation is related to the temporary potential energy storage in elastic structures and the rapid release of this energy to actuate the structure. SMHs exhibit the remarkable ability to undergo arbitrary temporary shape editing and subsequent shape recovery in response to external stimuli. To achieve this, the polymer structures of SMHs incorporate molecular switches that facilitate temporary shape editing. These switches are often integrated with pendant moieties, including short crystallizable side chains, oligomeric crystallizable side chains, complex-forming groups, or groups facilitating host-guest interactions. Through these design elements, various

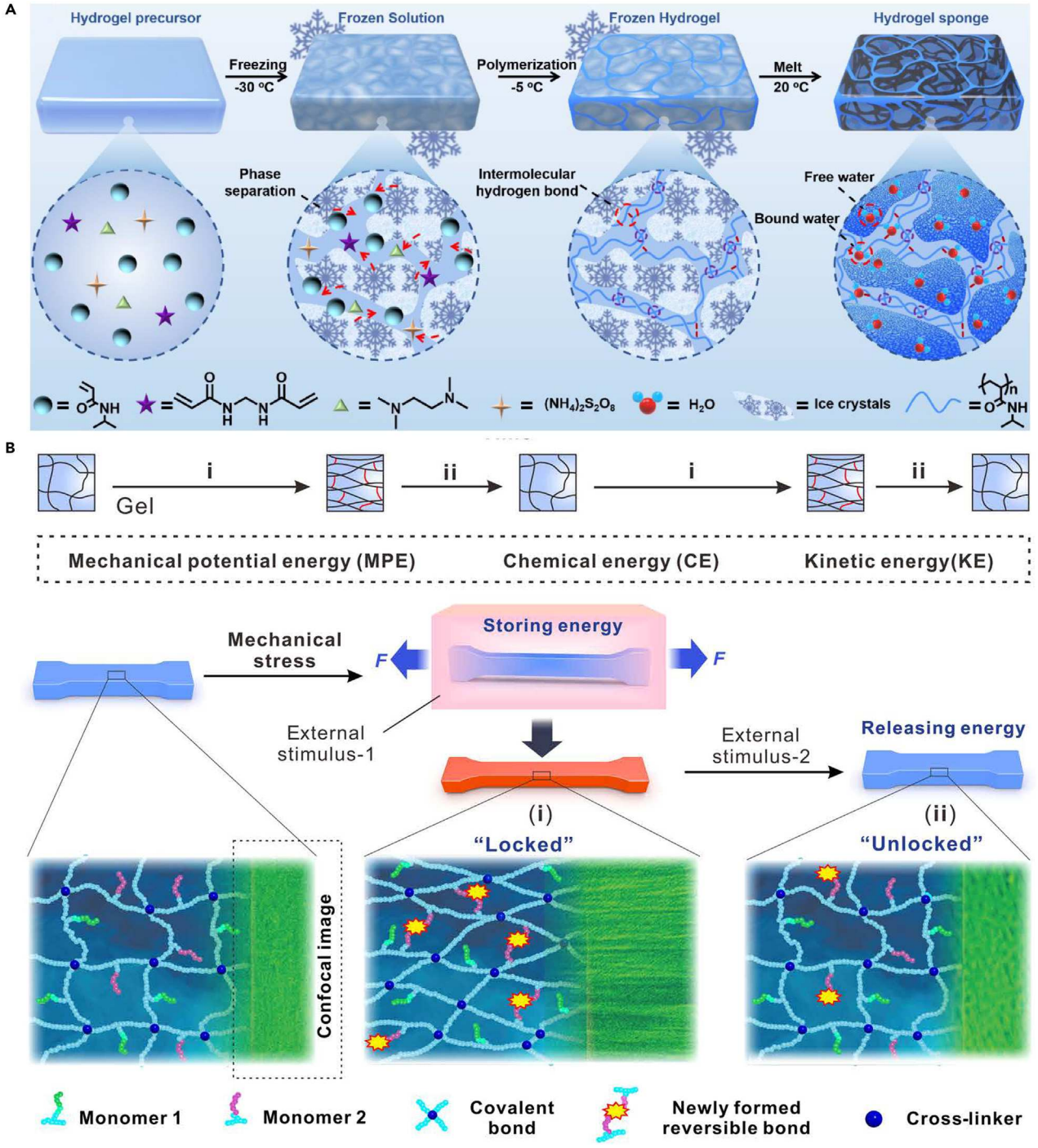

Figure 7. Strategies for osmotic pressure driven hydrogel actuators and elastic potential energy actuation of hydrogel actuators

(A) Schematic illustration of the thermal-induced deswelling principle of the PNIPAM sponge hydrogel and the ice-assisted synthesis of the hydrogel to increase the porosity. Reprinted with permission from Jian et al.[124] Copyright 2022, Elsevier.

(B) The elastic potential energy of the hydrogel network was used to achieve fast actuation based on the carboxylic-Fe^{3+} coordination. Reprinted with permission from Ma et al.[98] Copyright 2020, Science.

molecular mechanisms have been proposed to enable energy storage and release, thereby enabling shape-locking and shape-releasing processes.[130–132] It is important to note that the locking and release process in SMHs represents a programmable but nonreversible shape-shifting behavior. Once the final permanent shape is attained, it does not spontaneously revert to the temporary or locked shape unless an external force is applied during a reprogramming step.[133] For example, Lu et al.[134] fabricated a bilayer hydrogel, obtaining a thermo-responsive actuating layer and a shape-memory layer with metal ion response. The bilayer hydrogel could deform to a specific shape 1 by force and then be fixed by metal ion coordination. Subsequently, the hydrogel was placed in hot water at 60°C to deform into shape 2 as the PNIPAM hydrogel layer shrank. When the temperature of the external solution dropped to 15°C, the PNIPAM hydrogel layer expanded and the bilayer hydrogel was restored to shape 1. Finally, the hydrogel was soaked to remove metal complexation, restored to the initial shape, and used in the following shape programming.

Although the shifting pathway of SMH can be defined and altered in the programming procedure, the desirable energy storage and high work output related to high energy conversion efficiency are insufficient for SMH. This is mainly because of the weak reversible bonds and similar elastic moduli between the hydrogel locking and releasing states. In this case, most SMH actuators can only exhibit simple and moderate deformations such as bending, folding, and twisting. To improve the efficiency of energy storage and conversion of SMH, two fundamental strategies are considered: (1) strong reversible bonds to increase the energy storage content; and (2) high elasticity and noticeable elastic moduli difference between locking and releasing states of SMH to avoid excessive energy loss and improve the efficiency of energy conversion. Ma et al.[98] proposed an elastic energy storing and releasing method based on a P(AM-AA) hydrogel system. In the energy storage process, the hydrogel was stretched, and the shape was then locked by immersing the stretched hydrogel into an Fe^{3+} solution to form new carboxylic-Fe^{3+} coordination. Consequently, the explosive release can be achieved by UV light or acid solution to break the carboxylic-Fe^{3+} coordination (Figure 7B). This design strategy made the hydrogel generate high contractile force (40 kPa) rapidly at ultrahigh work density (15.3 kJ m^{-3}).

In addition, Hua et al.[104] prepared cold-induced SMHs based on the poly(acrylic acid)-calcium acetate (PAA-CaAc) systems. The storage modulus (G′) and loss modulus (G″) increased with increasing temperature from 35°C to 70°C, and G′ of the hydrogel could reach about 5.4 MPa at 70°C. The designed hydrogel could be fixed in different shapes at a high temperature, and a piece of hydrogel strip (0.5 g) with a temporary shape could support a load of 200 g. The unique shape-memory process enabled the bio-inspired artificial muscles to have an ultrahigh work density of 45.2 kJ m^{-3}, higher than that of biological muscles (~8 kJ m^{-3}). Thus, when compared to osmotic pressure actuation, elastic potential energy actuation offers advantages by eliminating the incompatibility between actuation force and response time. However, it is important to note that the energy storage process in elastic potential energy actuation can be relatively complex, time consuming, and dependent on the polymer structure. Moreover, as mentioned earlier, the shape editing and shape-recovery process in many cases is not reversible. Consequently, the design of hydrogels capable of programmable reversible shape deformation remains a challenge, limiting their application potential in a wider range of scenarios.

Responsive particle actuation

One approach of passive actuation to decouple the actuation force and response speed is incorporating responsive particles into hydrogels, which obtain a shorter response time of as low as 10^{-3} s under external stimuli.[16] The common responsive particles are magnetic particles, such as iron, Fe_3O_4, $MnFe_2O_4$, barium ferrite, carbonyl iron, nickel rods, and magnetite-coated alumina platelets,[29–34] responding to a magnetic field and free ions in ionic conductors responding to electric fields. The response time of hydrogel actuators based on responsive particle actuation mainly depends on the dimension and mechanical inertia of hydrogel carriers and the concentration of the responsive particles in hydrogel matrices.[105,135]

Anisotropic hydrogels incorporating magnetic particles often display nonuniform distribution of these particles, leading to uneven responsiveness and varying behaviors across different regions of the hydrogel.[136,137] As a result, the hydrogel exhibits unequal or distinct responsive characteristics in different areas. Moreover, the use of nonuniform magnetic fields to induce deformations in hydrogels that are proportional to the applied field gradient has been explored. This approach allows for precise control over the shape changes in the hydrogel based on the spatial variations of the magnetic field. For example, Simińska-Stanny et al.[40] printed patterned magnetic hydrogel models, such as tubes, cubes, and cantilevers, with different inks having different magnetic filler concentrations. The anisotropic hydrogels exhibited different shape- and pattern-dependent magnetic responses under a uniform magnetic field (Figure 8A). Tang et al.[41] employed the direct ink-printing method to fabricate hydrogels with hard magnetic NdFeB particles and then programmed magnetization on the hydrogel to adjust the distribution of NdFeB particles. Consequently, different parts of the hydrogel could generate a magnetic torque and collectively result in a complex shape when the magnetic polarities of magnetic particles were not aligning with the applied external magnetic field.

For an electric-field actuation, the electric field will induce bending deformations of the anionic/cationic hydrogels immersed in an aqueous solution containing a polyelectrolyte solute.[106,138] During the process, the migration of the polyelectrolyte solute under the electric field can result in the gradient concentration of the solute and difference in osmotic pressure between the hydrogel interior, which further achieves the hydrogels' deformation.[125,139] The actuation direction and intensity can be adjusted by changing the electric distribution and intensity, respectively. In addition, composite actuators were fabricated recently by embedding a dielectric elastomer membrane between two membranes made of hydrogel ionic conductors.[105] In this model, the application of voltage between the ionic conductors within the hydrogel led to the accumulation of oppositely charged ions on the surfaces of the hydrogel, which encased the dielectric elastomer. This accumulation of charges created an attractive force, resulting in the deformation of the sandwiched plate. As a consequence, the thickness of the plate decreased while the area simultaneously increased (Figure 8B). In contrast to hydrogels that rely on active actuation mechanisms, hydrogels actuated by responsive particles offer several advantages, including higher actuation speed and adjustable actuation force. However, achieving diverse and complex deformations of hydrogels in magnetic and electric fields remains a significant challenge. While advanced preparation methods such as 3D printing[135] and multi-layer assembly[106] have been utilized to program hydrogel structures and enhance their deformation capabilities, certain limitations persist. These include complex preparation procedures and limited control over the resulting structural characteristics. As a result, further research is necessary to overcome

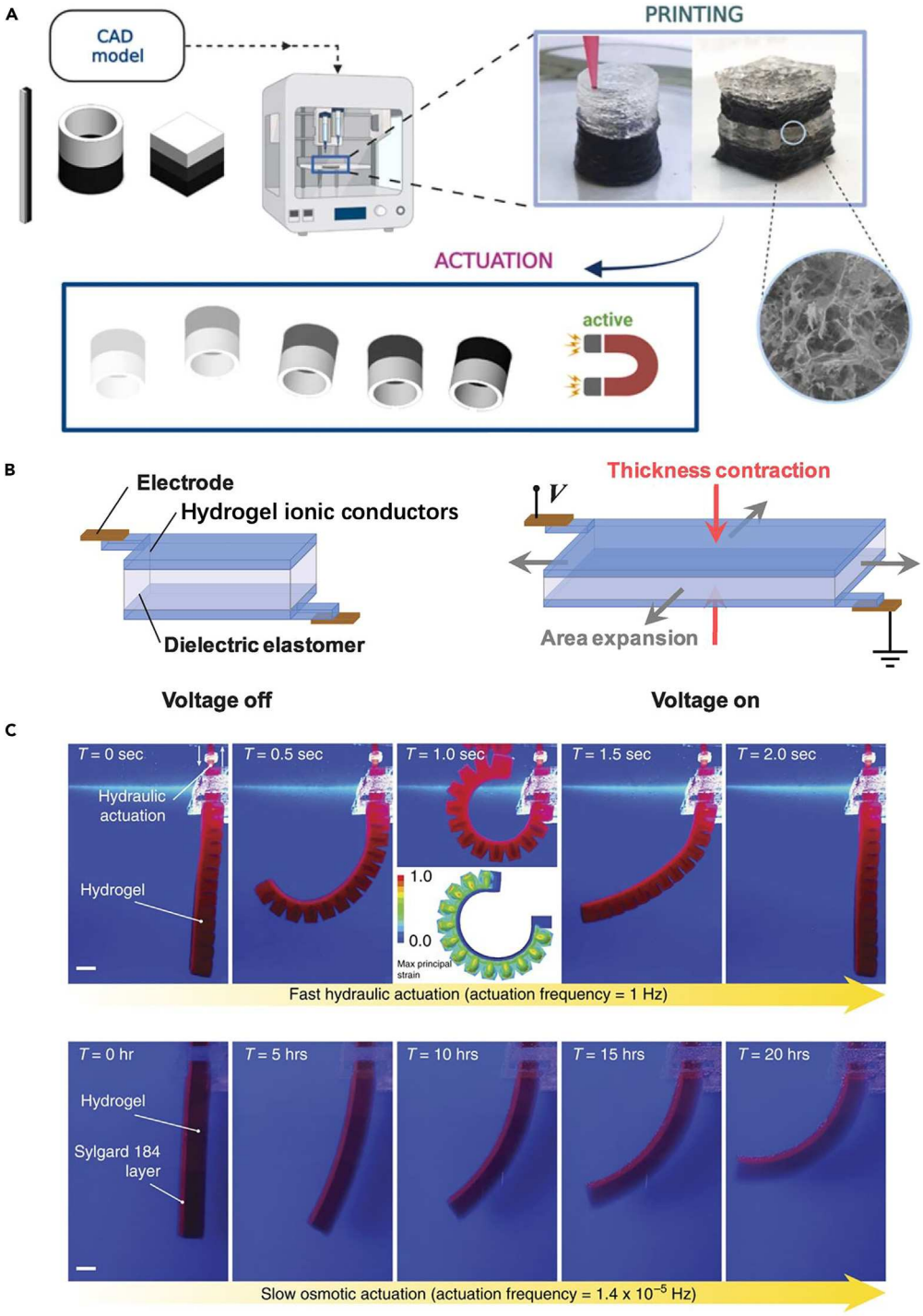

Figure 8. Responsive particle actuation and hydraulic/pneumatic actuation of hydrogel actuators

(A) Schematic illustration of the multi-material 3D printing of magnetically graded hydrogels for different actuation modes. Reprinted with permission from Simińska-Stanny et al.[40] Copyright 2022, Elsevier.

(B) Soft actuators made of two layers of a hydrogel ionic conductor and a sandwiched dielectric elastomer can be actuated under an electric field. Reprinted with permission from Keplinger et al.[105] Copyright 2013, Science.

(C) Schematic illustration of a complex hydrogel actuator that can be actuated by hydraulic pressures. Scale bar, 1 cm. Reprinted with permission from Yuk et al.[108] Copyright 2017, Nature.

these challenges and improve the preparation and controllability of hydrogel structures for enhanced deformation performance.

Pneumatic and hydraulic actuation

Pneumatic and hydraulic actuation has been widely used in developing hydrogel actuators and robots with high actuation force and fast response speed. Hydrogel actuators are usually composed of connected chambers or channels in hydrogel matrices, which can pump the gas or fluid in and out to generate necessary pneumatic or hydraulic pressure for actuation.[140,141] Therefore, as for the pneumatic or hydraulic hydrogel-based actuators, suitable mechanical properties, such as high antifatigue and stiffness, are needed to accommodate the actuation pressure under cyclic pneumatic or hydraulic actuation to avoid leakage or failure of the actuators. Recently, many approaches have been researched to improve the mechanical properties of hydrogels through establishing double-network hydrophobically associating topological networks, compressive annealing, physical enhancement, and addition of ions, which benefit the extension of a hydrogel's service life.[142,143] Besides, the chamber or channel structures and corresponding force distribution inside the matrix are commonly simulated to obtain the optimal solution, which is crucial to actuation performance. Recently, many bio-inspired hydrogel-based actuators have been designed on the basis of octopus tentacles, butterflies, and worms.[144,145] Yuk et al.[108] proposed the first hydraulic hydrogel actuator consisting of hydraulic chambers and channels made of tough hydrogels. This exhibited higher actuation force (over 1 N) and fast response speed (<1 s) than existing osmotic hydrogel actuators (Figure 8C). Wu et al.,[107] inspired by the hollow structures of blood vessels and bamboo, designed and fabricated complex 3D hollow hydrogels based on supramolecular interactions. In this work, gelatin and Ca^{2+} were assembled to form a core structure with different shapes, after which the alginate covered the core through the Ca^{2+}-alginate coordination. The alginate-based hollow hydrogels were further obtained by dissolving the gelation core in warm water. The designed hollow hydrogel structures could be assembled to achieve pneumatic and hydraulic actuation via the pumping and blowing process of air and water. Additionally, Liang et al.[83] designed a fatigue-resistant (high fatigue threshold over 1,500 J m^{-2}) hydrogel by a bidirectional freezing-casting process followed by compressive annealing. The excellent mechanical properties allowed the hydrogel to be applied as load-bearing components for underwater robots, such as cyclic stretching-retracting.

Yuk et al.[108] proposed a hydraulic-induced actuation force F evaluation from a constrained hydrogel block and the responsive time t scale as

$$F \propto \Delta P L^2, t \propto t_{ext}, \quad \text{(Equation 2)}$$

where ΔP, t_{ext}, and L are the pressure inside the hydrogel chamber, the response time related to an external system such as a pump to supply the pressure, and the typical dimension of the model block, respectively. Therefore, the actuation force and speed are decoupled in pneumatic and hydraulic actuation, which shows a higher value than those related to active actuation. Nevertheless, challenges persist in achieving robust joints between the hydrogel matrix, connection tube, and air/liquid pumps, primarily due to their weak compatibility. Furthermore, the mechanical properties of hydrogels pose limitations on the maximum actuation force that can be generated, in contrast to elastomer matrices such as Ecoflex, Elastosil, and Sylgard 184.[146,147] However, the inherent versatility and tunable physical/chemical properties of hydrogels make them promising candidates for designing actuators driven by pneumatic and hydraulic pressure. These features facilitate easy functionality and enable the development of tailored actuation systems.

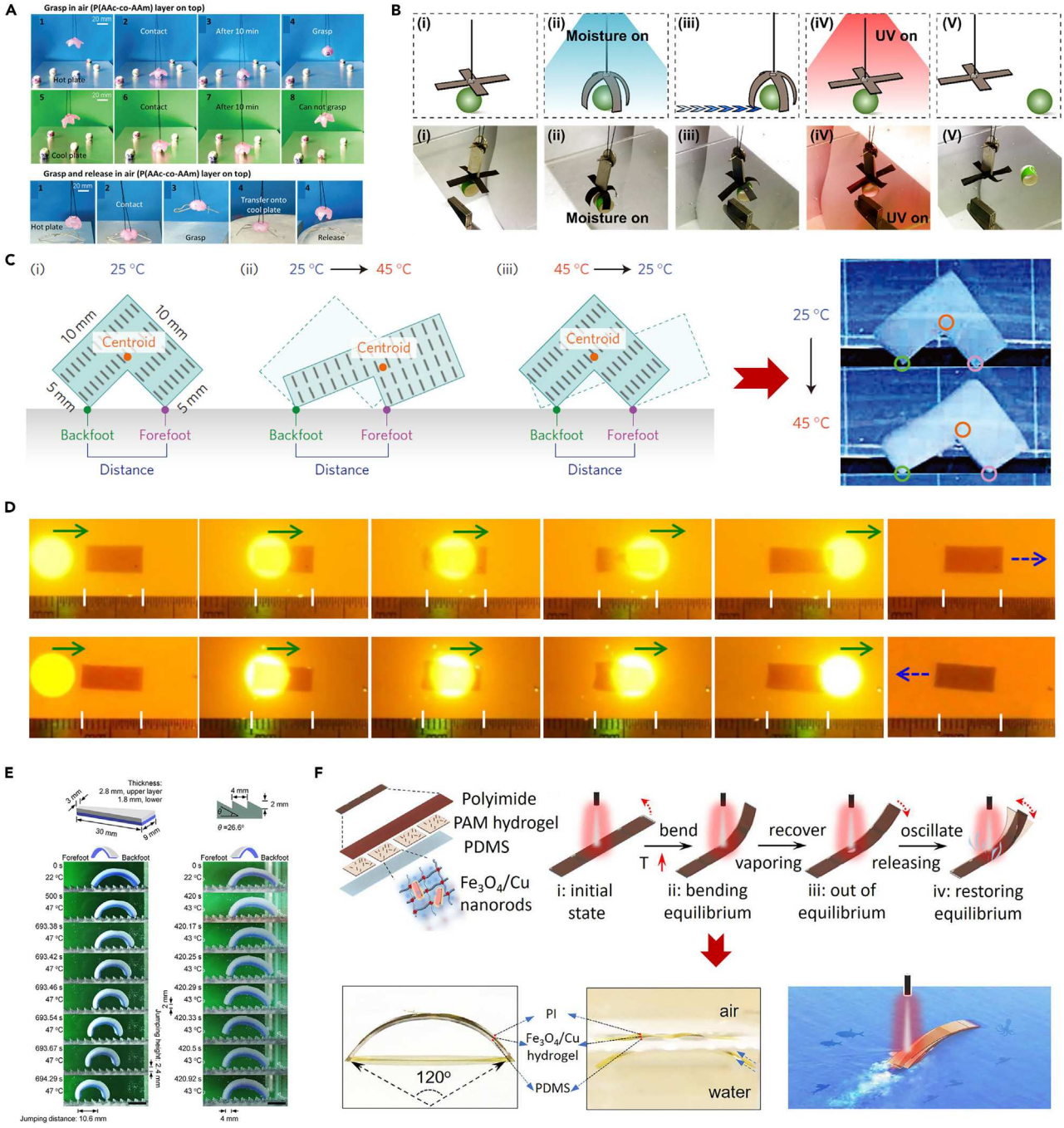

Figure 9. The applications of anisotropic hydrogels as grippers, walkers/crawlers, jumpers, and swimmers

(A) Hydrogel grippers were demonstrated to grasp and release objects under thermal actuation. Reprinted with permission from Zheng et al.[120] Copyright 2018, Royal Society of Chemistry.

(B) A smart hydrogel gripper can manipulate an object with humidity-, magnetic field-, and UV-based actuation. Reprinted with permission from Chathuranga et al.[148] Copyright 2022, American Chemical Society.

(C) An L-shaped symmetric PNIPA/TiNS hydrogel actuator can perform unidirectional procession. Reprinted with permission from Kim et al.[24] Copyright 2015, Nature.

(D) A slender hydrogel crawler moves forward under light actuation. Reprinted with permission from Zhu et al.[149] Copyright 2020, Nature.

Figure 9. *Continued*
(E) The bilayer hydrogel jumper can perform controlled jumping with the assistance of an aluminum ratchet. Reprinted with permission from Gao et al.[150] Copyright 2018, American Chemical Society.
(F) Schematic illustration of the structure and the working mechanism of a triple-layer hydrogel actuator driven by photothermal steam. Reprinted with permission from Li et al.[151] Copyright 2022, Science.

PROMISING APPLICATIONS OF ANISOTROPIC HYDROGELS IN SOFT ACTUATORS AND ROBOTS

Soft grippers

Anisotropic hydrogels have been widely used for developing soft grippers, which usually consist of three or more actuator fingers that can respond to external stimuli to achieve grasping or manipulations. For example, Zheng et al.[120] fabricated a mimosa-inspired bilayer hydrogel-based gripper with a pentagram shape, demonstrating the closing and reopening behaviors in different environments, such as water, paraffin, and air (Figure 9A). Sun et al.[152] prepared a photothermally responsive MXene nanocomposite hydrogel applied for soft manipulators. The bilayer anisotropic grippers with cross-shape could grasp and transfer the object under NIR illumination. In addition, Chathuranga et al.[148] designed a multi-stimulus-responsive hydrogel actuator consisting of graphene oxide, Fe_3O_4 nanoparticles, and tapioca starch via an evaporation-induced self-assembly method. This actuator was responsive to moisture gradient, magnetism, and UV light. When assembled as a gripper, it exhibited multi-responsive intelligence to perform object capture, movement, and release behaviors under moisture, magnetic, and UV fields (Figure 9B).

The soft grippers constructed from anisotropic hydrogels exhibited limited functionality, as they could only undergo unidirectional actuation in response to a single, uniform external stimulus. Reversing their bending motion required a considerable amount of time, either by removing the initial stimulus or by applying an opposing actuation force or strain. Consequently, these grippers faced challenges in achieving rapid and efficient capturing and releasing actions solely relying on osmotic pressure actuation under a single stimulus. Recently, we successfully fabricated a hydrogel-based gripper by introducing high-thermal-conductivity fillers (e.g., LM, boron nitride [BN], silicon nitride [Si_3N_4], aluminum nitride [AlN]) into PNIPAM hydrogels. Gravity-induced hydrogenation was used to generate the required gradient-distributed porous structure, thermal conductivity, and temperature response in the PNIPAM hydrogel. Under single continuous thermal actuation, the designed hydrogel-based gripper can exhibit multi-directional bending based on the synergistic effects of high-thermal-conductivity fillers on thermal conduction and water-discharge obstruction.[21,22] Therefore, the new hydrogel-based gripper can achieve both grasping and releasing continuously, providing a universal method for designing intelligent hydrogel-based grippers for further applications.

Walking/crawling robots

Hydrogels have also been used to build bio-inspired walking and crawling robots,[153] generally designed by controlling the asymmetrical shape and contact friction between hydrogel components. Strip-like models have been employed extensively as walkers or crawlers because of their simple implementation of repeated bending-unbending or extension-contraction behaviors under cyclic stimuli. In addition, specific substrates with rough or ratchet structures have been applied to facilitate the directional motion of hydrogel-based walkers. For example, Morales et al.[154] designed an electro-driven hydrogel-based walker consisting of cationic and anionic hydrogel legs and employed PDMS as the substrate. By adjusting the direction of

the electric field, the dual polyelectrolyte legs performed the opposite deformation in dilute salt solutions, and thus the fabricated hydrogel-based walkers could move forward. Kim et al.[24] developed an anisotropic L-shaped hydrogel walker that exhibited asymmetric frictions on the contact area due to the differently apportioned gravity. The L-shaped walkers demonstrated walking motions based on the isochoric deformation and asymmetric frictions through sequential heating-cooling stimuli (Figure 9C). Furthermore, bidirectional or omnidirectional motions can be achieved by modulating the frictions and hydrogel deformation. Zhu et al.[149] designed a bidirectional light-irradiated PNIPAM-based anisotropic crawler in which dynamic friction could be achieved by adjusting the adhesion and friction between the gel and substrate via the photothermal effect due to the hydrophilic-to-hydrophobic transition of the PNIPAM matrix. Thus, the crawlers could move forward under dynamic light irradiation (Figure 9D). They also proposed a stripe-patterned walker, in which the leg closer to the light had considerably more friction and served as an anchoring point to convert cyclic bending to directional walking.

Jumping robots

Hydrogel-based jumpers based on different structural designs and actuation types have been developed. They use a catapult-like energy conversion mechanism through which potential energy is temporarily stored in elastic structures, followed by the rapid release of this energy to complete the jump.[155] For example, Gao et al.[150] reported a snap-bucking motivated jumping of thermo-responsive bilayer hydrogel. The elastic energy of the thermo-responsive deformation could be constrained on the basis of adhesion between the hydrogels and aluminum ratchet. When the accumulated elastic energy overwhelmed the adhesion and the back foot snapped from the tooth, the hydrogel-based jumper jumped abruptly, and the jump direction, height, and distance were controlled by the design of the ratchet and hydrogel shape (Figure 9E). Recently, Lee et al.[156] fabricated a swelling-induced snap-bulking jumper with microgroove-containing double-curved gels as the legs. The double-curved hydrogels snapped and generated thrust to make the device jump off the ground upon solvent stimulation that swelled the gel near the grooves. However, continuous jumping behavior is still a major challenge because of the difficulty of continuous and reversible deformation under external stimuli.

Swimming robots

Hydrogel-based swimmers have been fabricated using different swimmer models and dynamic morphing under an external stimulus. For example, Zhang et al.[157] prepared an octopus-inspired light-driven hydrogel-based swimmer consisting of a bilayer strip structure. Under cyclic NIR, the hydrogel actuators performed shape bending and generated a propulsion force larger than the water drag force, resulting in the forward motion of the hydrogel swimmer. The propulsion and swimming speed are related to the NIR power and the size of the actuators. The water environment benefits hydrogel-based swimmers with a swelling and deswelling actuation mechanism, which can protect the functional integrity and provide the actuation power.

Recently, Li et al.[151] designed a light-powered soft oscillator with adaptive oscillation modes in response to light irradiation of different intensities. The soft oscillator had a hierarchical structure, and the critical actuation part was made of a photothermal actuator consisting of hydrogel and Fe_3O_4/Cu hybrid nanorods that could convert light to heat. The actuation part could generate steam by vaporizing the water in the porous hydrogels under NIR, acting as the power to actuate the hydrogel-based swimmer (Figure 9F). Besides, the water environment provided a

continuous water supply for the photothermal steam. The hydrogel was also designed to have load-bearing components for underwater robots based on cyclic stretching-retracting to generate propulsion by pushing the surrounding water backward like a jellyfish.[83]

Intelligent actuators and robots with multi-functionality

Inspired by nature, recent attention has been paid to integrating multiple functions, such as sensing, fluorescent, self-healing, or shape-memory properties, into hydrogel actuators to achieve intelligent hydrogel actuators with broader applications.[145,158–160] A self-sensitive actuating system based on responsive and conductive hydrogels has recently been developed.[73,93] To avoid the influence of the function interaction, the hydrogels are usually designed on the basis of photothermal properties to prevent the influence of direct thermal stimulus on sensing performance. For instance, Li et al.[93] proposed a bilayer CNTs-elastomer/PNIPAM composite, resembling the combination between skin and muscles, to achieve both shape morphing and sensing functions. Under NIR irradiation, the photothermal CNTs led to shrinking of the hydrogel layer due to water loss, and thereby the composite generated shape change. Meanwhile, the conductive layer consisting of CNTs-elastomer was conducive and generated the electrical signal due to deformation of the conductive layer. Therefore, feedback signals could be generated to sense the magnitude of actuation (Figure 10A). Zhao et al.[73] designed an anisotropic conductive PANI/PNIPAM hydrogel by the ice-templating method. The PANI served as conductive units, and PNIPAM supported the actuating behavior. The prepared hydrogel could curl up, grasp, and move an object with real-time motion sensing by monitoring the resistance change under the irradiation of NIR (Figure 10B). Furthermore, a closed-loop actuation system was designed to mimic a biological neuromuscular system based on combining sensory and actuating functions. In addition, attaching a soft physical sensor to the surface of soft actuators or robots can also achieve the accurate monitoring of actuation and sense different information, such as temperature and contact pressure.[163]

Additionally, fluorescence has been introduced into the actuation system to achieve dynamic optical camouflage under different conductions and has attracted tremendous attention. To accomplish the synergistic color-changing and shape-morphing capabilities, Wei et al.[164] combined fluorescence and actuation into a hydrogel system based on supramolecular dynamic metal-ligand coordination. The actuator's color could be changed correspondingly by controlling the environmental stimuli such as acidity/alkalinity change and metal ions. Besides this, reversible complex 3D deformations could be thermo-triggered, and chameleon-shaped soft hydrogel robots were fabricated to resemble the natural chameleons to achieve camouflage based on fluorescence and actuation behaviors. They also designed a supramolecular fluorescent polymeric hydrogel with the integrated properties of wide multi-color tunability, multi-responsiveness, and remolding capacities.[161] Multiple R/G/B fluorophores were organized into different polymer chains in the hydrogel matrix to achieve a multi-responsive multi-color fluorescence response, resembling the various appearances and color changes of living creatures responding to multiple environmental stimuli (Figure 10C). Recently, Li et al.[165] designed thermal camouflaging MXene skins that exhibited stimulus sensation and wireless communication based on the harnessing of interfacial instability and intrinsic Seebeck effect. The soft robot with the MXene skin was capable of adaptive thermal camouflage and recording its locomotion routes.

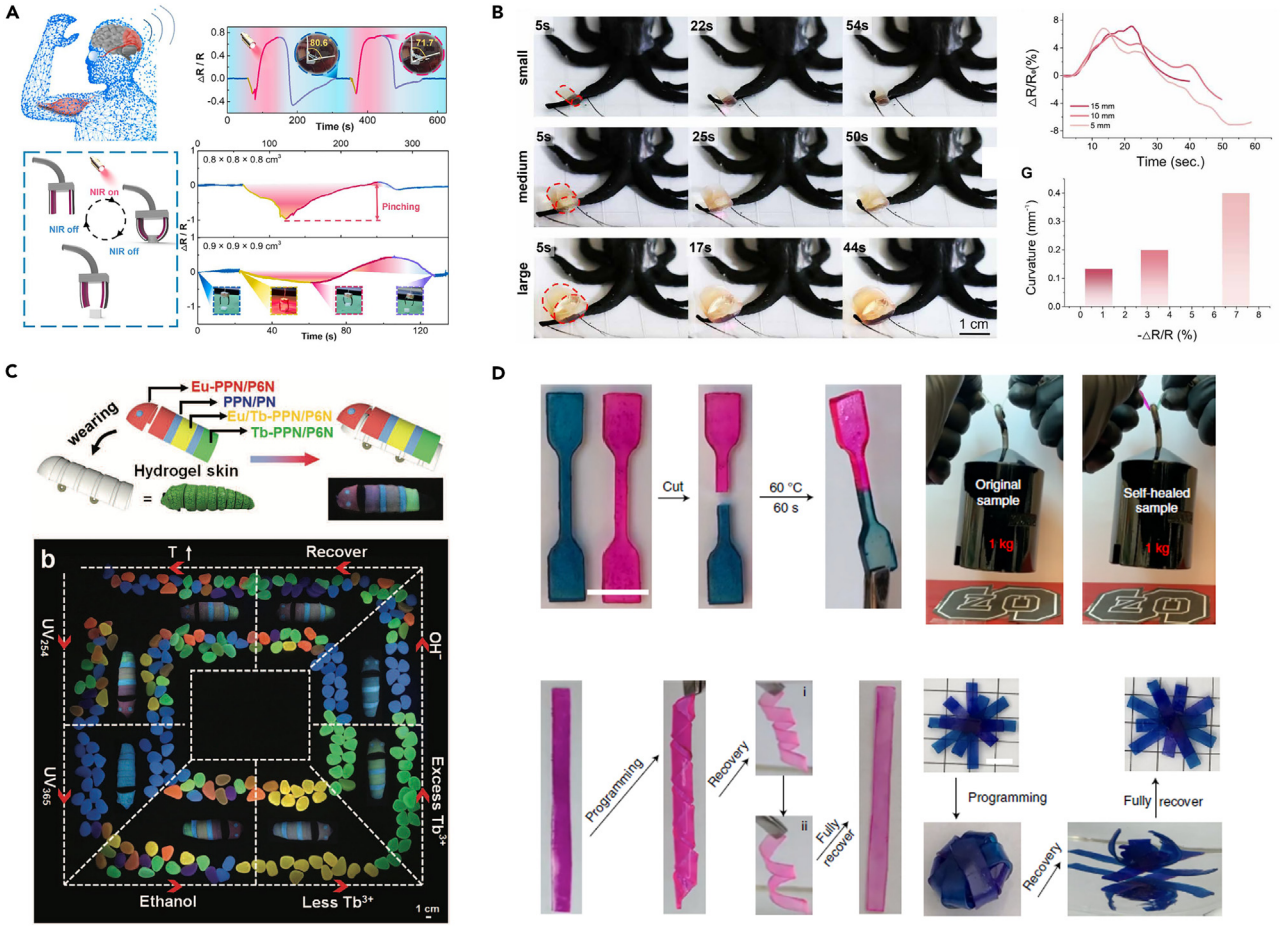

Figure 10. Intelligent actuators and robots with multi-functionality

(A and B) Intelligent hydrogel actuators capable of self-sensing. Reprinted with permission from Li et al.[93] Copyright 2021 Elsevier; Reprinted with permission from Zhao et al.[73] Copyright 2021, Science.

(C) Schematic illustration of a hydrogel robot integrated with fluorescence. Reprinted with permission from Liu et al.[161] Copyright 2022, Wiley-VCH.

(D) Intelligent actuators and robots with self-healing and shape-memory properties. Reprinted with permission from Wang et al.[162] Copyright 2022, Nature.

Based on the molecular design strategy, Jiang et al.[123] prepared a tough, self-healing hydrogel with ultrafast shape changing by introducing acid-ether hydrogen bonding and imine bonds into the hydrogel matrix. The self-healing efficiency reached 84% after 50 min without any external stimulus. Shape memory has also been introduced into the actuating hydrogel system to improve its shape programmability. Wang et al.[162] designed tough and stretchable ionogels by co-polymerizing acrylamide and acrylic acid in ionic liquid. Owing to the *in situ* phase separation and temperature-dependent phase behavior, the designed ionogels exhibited ~60% self-healing efficiency and shape-memory property with programming at a temperature higher than the glass transition temperature of 48.2°C and fixing at room temperature (Figure 10D). These strategies to design actuating hydrogels with other functions expand their potential applications and inspire the design of more intelligent hydrogel-based actuators.

CONCLUSION AND OUTLOOK

This review has summarized the recent advances in developing anisotropic hydrogels and their applications in soft actuators and robots. The primary design and

fabrication strategies for anisotropic hydrogels are categorized and discussed, including gravity-induced anisotropy, electric-field-induced anisotropy, magnetic-field-induced anisotropy, local-pattern-induced anisotropy, shear-flow-induced anisotropy, polymer-chain-alignment-induced anisotropy, and layered-structure-formed anisotropy. Moreover, the major actuation and control methods for anisotropic hydrogel-based soft actuators and robots are discussed with highlighted pros and cons. Additionally, the significant applications of the anisotropic hydrogels in soft actuators and soft robots, including soft grippers, walking/crawling robots, jumping robots, and swimming robots, are discussed in detail. Finally, special attention was is paid to the advanced intelligence of soft actuators with multi-functionality, which combines different material properties for specific applications to expand the potential applications of heterogeneous hydrogel-based actuators.

With the rapid progress of anisotropic hydrogels in soft actuators and robots, there are great opportunities but also significant challenges in the future roadmap of this research field. First, the mechanical properties (e.g., strength, toughness, and durability) and the response performance (e.g., actuation force and response speed) of the anisotropic hydrogels must be improved. Most current anisotropic hydrogels are prepared on the basis of a covalently crosslinked network, which usually has relatively poor mechanical properties due to weak intermolecular interactions and low energy dissipation under large deformations. As a result, the work or power density of the hydrogels is also relatively low. Several approaches have been developed to improve the mechanical properties of hydrogels, including double networks, topological networks, slide-ring structures, hydrophobic association, physical enhancement, chelation of metal ions, and salting-out effect. These methods should be combined to facilitate the development of anisotropic hydrogels for actuators and robots. Although several new techniques, such as phase separation, self-training, or 3D printing, have been proposed to design high-strength or tough hydrogels with anisotropic structures, the fabrication and material preparation is still expensive and time consuming. Therefore, more effort should be put into studying new fabrication approaches.

Second, the control and actuation methods should be improved, and coupling simulation models must be developed to accurately predict the deformation and behaviors. The nonlinear elasticity with strain-related stiffness is quite complex; thus, a better understanding of the responses of the hydrogel, especially under multi-physics stimuli, will be necessary to improve the control of hydrogel-based actuators and robots. It is noteworthy that the hydrogel actuators based on osmotic pressure actuation usually suffer from slow actuation speed. Their actuation force largely relies on the diffusion-limited uptake and release of water, strongly affected by the microstructure of hydrogels. A highly porous structure can facilitate water discharge to obtain a high actuation speed, but this results in poor mechanical properties due to the low density of polymer chains. Therefore, it is critical to develop advanced actuators by precisely controlling the pore structure in the fabrication steps and achieving a balance between mechanical properties and actuation speed. In this regard, the high energy storage and release efficiency in elastic potential energy actuation, the mechanical properties of the hydrogel matrix in pneumatic or hydraulic actuation, and the compatibility between responsive particles and hydrogels should be improved.

Multi-functional anisotropic hydrogels have become a new promising direction. However, it is still challenging to integrate biomimetic properties, such as self-healing and self-sensing, with hydrogels for broad applications because of the

incompatibility between the material properties of constituent phases and the diversity of working conditions. The responses of the multi-functional hydrogels under various stimuli and their interactions will be worth investigating to achieve advanced functional actuators. In addition, developing new compatible inks and materials for 3D/4D printing of hydrogel-based actuators and robots will be an essential research topic. The precise control of the anisotropic structure in the actuators and robots will enable the accurate control of deformation and actuation. Module design and integration of hydrogel blocks will be promising for the high-throughput production of advanced actuators and robots. However, for large actuators, the balance between actuation speed, actuation force, and energy efficiency must be considered for real applications.

Furthermore, it is crucial to address the challenges related to the high water-retention rate and packaging techniques of hydrogel actuators and robots in order to enhance their durability and environmental stability, particularly in harsh conditions involving dryness, heat, fire hazards, or toxic substances. To tackle these challenges, recent research has explored the use of composite actuators, which combine hydrogels with cryoprotectants, metal elastomers, or ionic liquids to improve actuation stability and adaptability in multiple environments.[166,167] However, in such composite designs it is essential to enhance the characteristics of different materials and, in particular, the interface bonding to achieve optimal performance and facilitate ease of integration. Enhancing these aspects will contribute to the overall performance and practicality of hydrogel-based actuators and robots in diverse environments.

In addition, the actuation performance of hydrogels, particularly those actuated by osmotic pressure, can be influenced by the introduction of cryoprotectants or ionic liquids. Exploring new strategies or modifications in this regard will be crucial for advancing their actuation capabilities. The modeling and manufacturing of anisotropic hydrogels also play a vital role in their practical applications.[168] Although significant progress has been made in the study and application of anisotropic hydrogels in soft actuators, the development of hydrogel-based actuators or robots is still in its early stages and cannot be directly applied in real-world scenarios. Mathematical and physical modeling approaches can enhance our understanding and aid in the design of different hydrogel systems.

Finally, integrating actuation, sensing, control, and communication functionalities is a key focus in the design of robotic hydrogels.[160,169–172] This holistic approach allows for the development of multi-functional systems. Apart from actuation, anisotropic hydrogels have found application in various bio-fields. They have been used in miniature soft robots/actuators with therapeutic and diagnostic functions[173,174] as well as hydrogel-based patches or dressings for tissue engineering.[175,176] These diverse applications highlight the potential of anisotropic hydrogels beyond the actuation domain.

In conclusion, the field of multi-phasic anisotropic hydrogel research is rapidly advancing, presenting numerous significant challenges. However, these challenges can be successfully overcome through cross-disciplinary collaboration, leveraging the expertise in computational materials science, chemical synthesis, and advanced manufacturing. By combining these diverse areas of knowledge, researchers can effectively explore the vast capabilities and applications of anisotropic actuating hydrogels. Furthermore, this collaborative effort can facilitate the translation of conceptual ideas into tangible commercialized products, offering solutions to real-world challenges in various domains, including medicine, energy, sustainability,

and manufacturing. The collective efforts of researchers from different disciplines hold great potential for driving the progress and practical implementation of anisotropic hydrogels in addressing global challenges.

ACKNOWLEDGMENTS

This work is partially supported by the Natural Science Foundation of China (no. 52273078 and no. 11704244). H.W. and C.C. acknowledge financial support from NSF (ECCS-2024649) and Case Western Reserve University.

AUTHOR CONTRIBUTIONS

Conceptualization, C.C., Z.C., and Y. Cheng; writing – original draft, Z.C. and C.C.; writing – review & editing, Z.C., H.W., Y. Cao, Y. Cheng, O.A., H.L., and C.C.; supervision, C.C. and Y.C.

DECLARATION OF INTERESTS

The authors declare no competing interests.

REFERENCES

1. Wang, Y., Li, J., Li, Y., and Yang, B. (2021). Biomimetic bioinks of nanofibrillar polymeric hydrogels for 3D bioprinting. Nano Today *39*, 101180. https://doi.org/10.1016/j.nantod.2021.101180.

2. Cheng, F.-m., Chen, H.-x., and Li, H.-d. (2021). Recent progress on hydrogel actuators. J. Mater. Chem. B *9*, 1762–1780. https://doi.org/10.1039/D0TB02524K.

3. Chen, Y., Hao, Y., Mensah, A., Lv, P., and Wei, Q. (2022). Bio-inspired hydrogels with fibrous structure: A review on design and biomedical applications. Biomater. Adv. *136*, 212799. https://doi.org/10.1016/j.bioadv.2022.212799.

4. Shang, J., Le, X., Zhang, J., Chen, T., and Theato, P. (2019). Trends in polymeric shape memory hydrogels and hydrogel actuators. Polym. Chem. *10*, 1036–1055. https://doi.org/10.1039/C8PY01286E.

5. Wei, J., Li, R., Li, L., Wang, W., and Chen, T. (2022). Touch-Responsive Hydrogel for Biomimetic Flytrap-Like Soft Actuator. Nano-Micro Lett. *14*, 182. https://doi.org/10.1007/s40820-022-00931-4.

6. Cui, J., Chen, J., Ni, Z., Dong, W., Chen, M., and Shi, D. (2022). High-Sensitivity Flexible Sensor Based on Biomimetic Strain-Stiffening Hydrogel. ACS Appl. Mater. Interfaces *14*, 47148–47156. https://doi.org/10.1021/acsami.2c15203.

7. Wei, H., Zhang, B., Lei, M., Lu, Z., Liu, J., Guo, B., and Yu, Y. (2022). Visible-Light-Mediated Nano-biomineralization of Customizable Tough Hydrogels for Biomimetic Tissue Engineering. ACS Nano *16*, 4734–4745. https://doi.org/10.1021/acsnano.1c11589.

8. Yang, Y., Li, B., Wu, N., Liu, W., Zhao, S., Zhang, C.J., Liu, J., and Zeng, Z. (2022). Biomimetic Porous MXene-Based Hydrogel for High-Performance and Multifunctional Electromagnetic Interference Shielding. ACS Mater. Lett. *4*, 2352–2361. https://doi.org/10.1021/acsmaterialslett.2c00778.

9. Wang, H.-X., Zhao, X.-Y., Jiang, J.-Q., Liu, Z.-T., Liu, Z.-W., and Li, G. (2022). Thermal-Responsive Hydrogel Actuators with Photo-Programmable Shapes and Actuating Trajectories. ACS Appl. Mater. Interfaces *14*, 51244–51252. https://doi.org/10.1021/acsami.2c11514.

10. Coyle, S., Majidi, C., LeDuc, P., and Hsia, K.J. (2018). Bio-inspired soft robotics: Material selection, actuation, and design. Extreme Mechanics Letters *22*, 51–59. https://doi.org/10.1016/j.eml.2018.05.003.

11. Lin, X., Wang, Z., Jia, X., Chen, R., Qin, Y., Bian, Y., Sheng, W., Li, S., and Gao, Z. (2023). Stimulus-responsive hydrogels: A potent tool for biosensing in food safety. Trends Food Sci. Technol. *131*, 91–103. https://doi.org/10.1016/j.tifs.2022.12.002.

12. Yang, D. (2022). Recent Advances in Hydrogels. Chem. Mater. *34*, 1987–1989. https://doi.org/10.1021/acs.chemmater.2c00188.

13. Chen, M., Cui, Y., Wang, Y., and Chang, C. (2023). Triple physically cross-linked hydrogel artificial muscles with high-stroke and high-work capacity. Chem. Eng. J. *453*, 139893. https://doi.org/10.1016/j.cej.2022.139893.

14. Luo, C., Huang, M., Sun, X., Wei, N., Shi, H., Li, H., Lin, M., and Sun, J. (2022). Super-Strong, Nonswellable, and Biocompatible Hydrogels Inspired by Human Tendons. ACS Appl. Mater. Interfaces *14*, 2638–2649. https://doi.org/10.1021/acsami.1c23102.

15. Ying, B., and Liu, X. (2021). Skin-like hydrogel devices for wearable sensing, soft robotics and beyond. iScience *24*, 103174. https://doi.org/10.1016/j.isci.2021.103174.

16. Liu, X., Liu, J., Lin, S., and Zhao, X. (2020). Hydrogel machines. Mater. Today *36*, 102–124. https://doi.org/10.1016/j.mattod.2019.12.026.

17. Peng, X., and Wang, H. (2018). Shape changing hydrogels and their applications as soft actuators. J. Polym. Sci., Part B: Polym. Phys. *56*, 1314–1324. https://doi.org/10.1002/polb.24724.

18. Sano, K., Ishida, Y., and Aida, T. (2018). Synthesis of Anisotropic Hydrogels and Their Applications. Angew Chem. Int. Ed. Engl. *57*, 2532–2543. https://doi.org/10.1002/anie.201708196.

19. Jiao, D., Zhu, Q.L., Li, C.Y., Zheng, Q., and Wu, Z.L. (2022). Programmable Morphing Hydrogels for Soft Actuators and Robots: From Structure Designs to Active Functions. Acc. Chem. Res. *55*, 1533–1545. https://doi.org/10.1021/acs.accounts.2c00046.

20. Luo, R., Wu, J., Dinh, N.-D., and Chen, C.-H. (2015). Gradient Porous Elastic Hydrogels with Shape-Memory Property and Anisotropic Responses for Programmable Locomotion. Adv. Funct. Mater. *25*, 7272–7279. https://doi.org/10.1002/adfm.201503434.

21. Chen, Y., Chen, Z., Chen, C., Ur Rehman, H., Liu, H., Li, H., and Hedenqvist, M.S. (2021). A gradient-distributed liquid-metal hydrogel capable of tunable actuation. Chem. Eng. J. *421*, 127762. https://doi.org/10.1016/j.cej.2020.127762.

22. Chen, Z., Chen, Y., Chen, C., Zheng, X., Li, H., and Liu, H. (2021). Dual-gradient PNIPAM-based hydrogel capable of rapid response and tunable actuation. Chem. Eng. J. *424*, 130562. https://doi.org/10.1016/j.cej.2021.130562.

23. Ren, Y., Liu, Z., Jin, G., Yang, M., Shao, Y., Li, W., Wu, Y., Liu, L., and Yan, F. (2021). Electric-Field-Induced Gradient Ionogels for Highly Sensitive, Broad-Range-Response, and Freeze/Heat-Resistant Ionic Fingers. Adv. Mater. *33*, 2008486. https://doi.org/10.1002/adma.202008486.

24. Kim, Y.S., Liu, M., Ishida, Y., Ebina, Y., Osada, M., Sasaki, T., Hikima, T., Takata, M., and Aida, T. (2015). Thermoresponsive actuation enabled by permittivity switching in an electrostatically anisotropic hydrogel. Nat. Mater. *14*, 1002–1007. https://doi.org/10.1038/nmat4363.

25. Chen, Y., Liu, Y., Xia, Y., Liu, X., Qiang, Z., Yang, J., Zhang, B., Hu, Z., Wang, Q., Wu, W., et al. (2020). Electric Field-Induced Assembly and Alignment of Silver-Coated Cellulose for Polymer Composite Films with Enhanced Dielectric Permittivity and Anisotropic Light Transmission. ACS Appl. Mater. Interfaces *12*, 24242–24249. https://doi.org/10.1021/acsami.0c03086.

26. Chen, Y., Ding, Z., Wu, Y., Chen, Q., Liu, M., Yu, H., Wang, D., Zhang, Y., and Wang, T. (2019). Nanoscale magnetization reversal by electric field-induced ion migration. Biomolecules *10*, 14–26. https://doi.org/10.1557/mrc.2018.191.

27. Yang, C., Shi, X., Deng, H., and Du, Y. (2022). Antifatigue Hydration-Induced Polysaccharide Hydrogel Actuators Inspired by Crab Joint Wrinkles. ACS Appl. Mater. Interfaces *14*, 6251–6260. https://doi.org/10.1021/acsami.1c24430.

28. Xue, P., Bisoyi, H.K., Chen, Y., Zeng, H., Yang, J., Yang, X., Lv, P., Zhang, X., Priimagi, A., Wang, L., et al. (2021). Near-Infrared Light-Driven Shape-Morphing of Programmable Anisotropic Hydrogels Enabled by MXene Nanosheets. Angew Chem. Int. Ed. Engl. *60*, 3390–3396. https://doi.org/10.1002/anie.202014533.

29. Liu, K., Pan, X., Chen, L., Huang, L., Ni, Y., Liu, J., Cao, S., and Wang, H. (2018). Ultrasoft Self-Healing Nanoparticle-Hydrogel Composites with Conductive and Magnetic Properties. ACS Sustain. Chem. Eng. *6*, 6395–6403. https://doi.org/10.1021/acssuschemeng.8b00193.

30. Guo, R., Sun, X., Yuan, B., Wang, H., and Liu, J. (2019). Magnetic Liquid Metal (Fe-EGaIn) Based Multifunctional Electronics for Remote Self-Healing Materials, Degradable Electronics, and Thermal Transfer Printing. Adv. Sci. *6*, 1901478. https://doi.org/10.1002/advs.201901478.

31. Li, Y.P., Liang, Z.L., Gao, Q., Huang, L.R., Mao, Q.Y., Wen, S.Q., Liu, Y., Yin, W.D., Li, R.C., and Wang, J.Z. (2012). Programmable responsive shaping behavior induced by visible multi-dimensional gradients of magnetic nanoparticles. Vaccine X. *30*, 3295–3303. https://doi.org/10.1039/C2SM07206H.

32. Yan, X., Sun, T., Song, Y., Peng, W., Xu, Y., Luo, G., Li, M., Chen, S., Fang, W.-W., Dong, L., et al. (2022). In situ Thermal-Responsive Magnetic Hydrogel for Multidisciplinary Therapy of Hepatocellular Carcinoma. Nano Lett. *22*, 2251–2260. https://doi.org/10.1021/acs.nanolett.1c04413.

33. Daya, R., Xu, C., Nguyen, N.-Y.T., and Liu, H.H. (2022). Angiogenic Hyaluronic Acid Hydrogels with Curcumin-Coated Magnetic Nanoparticles for Tissue Repair. ACS Appl. Mater. Interfaces *14*, 11051–11067. https://doi.org/10.1021/acsami.1c19889.

34. Ma, Y., Ma, A., Luo, T., Xiao, S., and Zhou, H. (2023). Fabrication of anisotropic nanocomposite hydrogels by magnetic field-induced orientation for mimicking cardiac tissue. J. Appl. Polym. Sci. *140*, e53248. https://doi.org/10.1002/app.53248.

35. Goudu, S.R., Yasa, I.C., Hu, X., Ceylan, H., Hu, W., and Sitti, M. (2020). Biodegradable Untethered Magnetic Hydrogel Milli-Grippers. Adv. Funct. Mater. *30*, 2004975. https://doi.org/10.1002/adfm.202004975.

36. Gong, C., Zhai, Y., Zhou, J., Wang, Y., and Chang, C. (2022). Magnetic field assisted fabrication of asymmetric hydrogels for complex shape deformable actuators. J. Mater. Chem. C Mater. *10*, 549–556. https://doi.org/10.1039/D1TC04790F.

37. Sano, K., Arazoe, Y.O., Ishida, Y., Ebina, Y., Osada, M., Sasaki, T., Hikima, T., and Aida, T. (2018). Extra-Large Mechanical Anisotropy of a Hydrogel with Maximized Electrostatic Repulsion between Cofacially Aligned 2D Electrolytes. Angew Chem. Int. Ed. Engl. *57*, 12508–12513. https://doi.org/10.1002/anie.201807240.

38. Tang, J., Yin, Q., Qiao, Y., and Wang, T. (2019). Shape Morphing of Hydrogels in Alternating Magnetic Field. ACS Appl. Mater. Interfaces *11*, 21194–21200. https://doi.org/10.1021/acsami.9b05742.

39. Tang, J., Yin, Q., Shi, M., Yang, M., Yang, H., Sun, B., Guo, B., and Wang, T. (2021). Programmable shape transformation of 3D printed magnetic hydrogel composite for hyperthermia cancer therapy. Extreme Mechanics Letters *46*, 101305. https://doi.org/10.1016/j.eml.2021.101305.

40. Simińska-Stanny, J., Nizioł, M., Szymczyk-Ziółkowska, P., Brożyna, M., Junka, A., Shavandi, A., and Podstawczyk, D. (2022). 4D printing of patterned multimaterial magnetic hydrogel actuators. Addit. Manuf. *49*, 102506. https://doi.org/10.1016/j.addma.2021.102506.

41. Tang, J., Sun, B., Yin, Q., Yang, M., Hu, J., and Wang, T. (2021). 3D printable, tough, magnetic hydrogels with programmed magnetization for fast actuation. J. Mater. Chem. B *9*, 9183–9190. https://doi.org/10.1039/D1TB01694F.

42. Zhang, L., Guan, X., Xiao, X., Chen, Z., Zhou, G., and Fan, Y. (2022). Dual-phase injectable thermosensitive hydrogel incorporating Fe3O4@PDA with pH and NIR triggered drug release for synergistic tumor therapy. Eur. Polym. J. *176*, 111424. https://doi.org/10.1016/j.eurpolymj.2022.111424.

43. Hu, S., Zheng, M., Wang, Q., Li, L., Xing, J., Chen, K., Qi, F., He, P., Mao, L., Shi, Z., et al. (2022). Cellulose hydrogel-based biodegradable and recyclable magnetoelectric composites for electromechanical conversion. Carbohydr. Polym. *298*, 120115. https://doi.org/10.1016/j.carbpol.2022.120115.

44. Mahdi Eshaghi, M., Pourmadadi, M., Rahdar, A., and Díez-Pascual, A.M. (2022). Novel Carboxymethyl Cellulose-Based Hydrogel with Core–Shell Fe3O4@SiO2 Nanoparticles for Quercetin Delivery. Materials *15*, 8711.

45. Armon, S., Efrati, E., Kupferman, R., and Sharon, E. (2011). Geometry and Mechanics in the Opening of Chiral Seed Pods. Science *333*, 1726–1730. https://doi.org/10.1126/science.1203874.

46. Dai, C.F., Khoruzhenko, O., Zhang, C., Zhu, Q.L., Jiao, D., Du, M., Breu, J., Zhao, P., Zheng, Q., and Wu, Z.L. (2022). Magneto-Orientation of Magnetic Double Stacks for Patterned Anisotropic Hydrogels with Multiple Responses and Modulable Motions. Angew Chem. Int. Ed. Engl. *61*, e202207272. https://doi.org/10.1002/anie.202207272.

47. Liu, J., Jiang, L., Liu, A., He, S., and Shao, W. (2022). Ultrafast thermo-responsive bilayer hydrogel actuator assisted by hydrogel microspheres. Sensor. Actuator. B Chem. *357*, 131434. https://doi.org/10.1016/j.snb.2022.131434.

48. Wang, Z.J., Hong, W., Wu, Z.L., and Zheng, Q. (2017). Site-Specific Pre-Swelling-Directed Morphing Structures of Patterned Hydrogels. Angew Chem. Int. Ed. Engl. *56*, 15974–15978. https://doi.org/10.1002/anie.201708926.

49. Hua, L., Xie, M., Jian, Y., Wu, B., Chen, C., and Zhao, C. (2019). Multiple-Responsive and Amphibious Hydrogel Actuator Based on Asymmetric UCST-Type Volume Phase Transition. ACS Appl. Mater. Interfaces *11*, 43641–43648. https://doi.org/10.1021/acsami.9b17159.

50. Xu, Z., and Fu, J. (2020). Programmable and Reversible 3D-/4D-Shape-Morphing Hydrogels with Precisely Defined Ion Coordination. ACS Appl. Mater. Interfaces *12*, 26476–26484. https://doi.org/10.1021/acsami.0c06342.

51. Kim, J., Hanna, J.A., Byun, M., Santangelo, C.D., and Hayward, R.C. (2012). Designing Responsive Buckled Surfaces by Halftone Gel Lithography. Science *335*, 1201–1205. https://doi.org/10.1126/science.1215309.

52. Fadeev, M., Davidson-Rozenfeld, G., Biniuri, Y., Yakobi, R., Cazelles, R., Aleman-Garcia, M.A., and Willner, I. (2018). Redox-triggered hydrogels revealing switchable stiffness properties and shape-memory functions. Polym. Chem. *9*, 2905–2912. https://doi.org/10.1039/C8PY00515J.

53. Yu, P., Li, Y., Sun, H., Ke, X., Xing, J., Zhao, Y., Xu, X., Qin, M., Xie, J., and Li, J. (2022). Cartilage-Inspired Hydrogel with Mechanical Adaptability, Controllable Lubrication, and Inflammation Regulation Abilities. ACS Appl. Mater. Interfaces *14*, 27360–27370. https://doi.org/10.1021/acsami.2c04609.

54. Palleau, E., Morales, D., Dickey, M.D., and Velev, O.D. (2013). Reversible patterning and actuation of hydrogels by electrically assisted ionoprinting. Nat. Commun. *4*, 2257. https://doi.org/10.1038/ncomms3257.

55. Peng, X., Li, Y., Zhang, Q., Shang, C., Bai, Q.-W., and Wang, H. (2016). Tough Hydrogels with Programmable and Complex Shape Deformations by Ion Dip-Dyeing and Transfer Printing. Adv. Funct. Mater. *26*, 4491–4500. https://doi.org/10.1002/adfm.201601389.

56. Sun, W., Schaffer, S., Dai, K., Yao, L., Feinberg, A., and Webster-Wood, V. (2021). 3D Printing Hydrogel-Based Soft and Biohybrid Actuators: A Mini-Review on Fabrication Techniques, Applications, and Challenges. Front. Robot. AI *8*, 673533. https://doi.org/10.3389/frobt.2021.673533.

57. Zhang, A., Wang, F., Chen, L., Wei, X., Xue, M., Yang, F., and Jiang, S. (2021). 3D printing hydrogels for actuators: A review. Chin.

Chem. Lett. *32*, 2923–2932. https://doi.org/10.1016/j.cclet.2021.03.073.

58. Puza, F., and Lienkamp, K. (2022). 3D Printing of Polymer Hydrogels—From Basic Techniques to Programmable Actuation. Adv. Funct. Mater. *32*, 2205345. https://doi.org/10.1002/adfm.202205345.

59. Gevorkian, A., Morozova, S.M., Kheiri, S., Khuu, N., Chen, H., Young, E., Yan, N., and Kumacheva, E. (2021). Actuation of Three-Dimensional-Printed Nanocolloidal Hydrogel with Structural Anisotropy. Adv. Funct. Mater. *31*, 2010743. https://doi.org/10.1002/adfm.202010743.

60. Zheng, S.Y., Shen, Y., Zhu, F., Yin, J., Qian, J., Fu, J., Wu, Z.L., and Zheng, Q. (2018). Programmed Deformations of 3D-Printed Tough Physical Hydrogels with High Response Speed and Large Output Force. Adv. Funct. Mater. *28*, 1803366. https://doi.org/10.1002/adfm.201803366.

61. Son, H., Byun, E., Yoon, Y.J., Nam, J., Song, S.H., and Yoon, C. (2020). Untethered Actuation of Hybrid Hydrogel Gripper via Ultrasound. ACS Macro Lett. *9*, 1766–1772. https://doi.org/10.1021/acsmacrolett.0c00702.

62. Zhu, W., Li, J., Leong, Y.J., Rozen, I., Qu, X., Dong, R., Wu, Z., Gao, W., Chung, P.H., Wang, J., and Chen, S. (2015). 3D-Printed Artificial Microfish. Adv. Mater. *27*, 4411–4417. https://doi.org/10.1002/adma.201501372.

63. Gladman, A.S., Matsumoto, E.A., Nuzzo, R.G., Mahadevan, L., and Lewis, J.A. (2016). Biomimetic 4D printing. Nat. Mater. *15*, 413–418. https://doi.org/10.1038/nmat4544.

64. Hu, X., Ge, Z., Wang, X., Jiao, N., Tung, S., and Liu, L. (2022). Multifunctional thermo-magnetically actuated hybrid soft millirobot based on 4D printing. Compos. B Eng. *228*, 109451. https://doi.org/10.1016/j.compositesb.2021.109451.

65. Shiblee, M.N.I., Ahmed, K., Kawakami, M., and Furukawa, H. (2019). 4D Printing of Shape-Memory Hydrogels for Soft-Robotic Functions. Adv. Mater. Technol. *4*, 1900071. https://doi.org/10.1002/admt.201900071.

66. Zhang, X.N., Zheng, Q., and Wu, Z.L. (2022). Recent advances in 3D printing of tough hydrogels: A review. Compos. B Eng. *238*, 109895. https://doi.org/10.1016/j.compositesb.2022.109895.

67. Chen, T., Bakhshi, H., Liu, L., Ji, J., and Agarwal, S. (2018). Combining 3D Printing with Electrospinning for Rapid Response and Enhanced Designability of Hydrogel Actuators. Adv. Funct. Mater. *28*, 1800514. https://doi.org/10.1002/adfm.201800514.

68. Cui, C., An, L., Zhang, Z., Ji, M., Chen, K., Yang, Y., Su, Q., Wang, F., Cheng, Y., and Zhang, Y. Reconfigurable 4D Printing of Reprocessable and Mechanically Strong Polythiourethane Covalent Adaptable Networks. Adv. Funct. Mater. n/a, 2203720. 10.1002/adfm.202203720.

69. Dong, Y., Wang, S., Ke, Y., Ding, L., Zeng, X., Magdassi, S., and Long, Y. (2020). 4D Printed Hydrogels: Fabrication, Materials, and Applications. Adv. Mater. Technol. *5*, 2000034. https://doi.org/10.1002/admt.202000034.

70. Zhao, Y., Zhou, T., Chen, X., Zhang, X., Peng, Z., Zhang, Y., Alsaid, Y., Frenkel, I., Youssef, K., Pei, Q., and He, X. (2020). Hierarchically Structured Stretchable Conductive Hydrogels for High-Performance Wearable Strain Sensors and Supercapacitors. Matter *5*, 1196–1197. https://doi.org/10.1016/j.matt.2020.08.024.

71. Feng, Y., Liu, H., Zhu, W., Guan, L., Yang, X., Zvyagin, A.V., Zhao, Y., Shen, C., Yang, B., and Lin, Q. (2021). Muscle-Inspired MXene Conductive Hydrogels with Anisotropy and Low-Temperature Tolerance for Wearable Flexible Sensors and Arrays. Adv. Funct. Mater. *31*, 2105264. https://doi.org/10.1002/adfm.202105264.

72. Miao, S., Wang, Y., Sun, L., and Zhao, Y. (2022). Freeze-derived heterogeneous structural color films. Nat. Commun. *13*, 4044. https://doi.org/10.1038/s41467-022-31717-2.

73. Zhao, Y., Lo, C.-Y., Ruan, L., Pi, C.-H., Kim, C., Alsaid, Y., Frenkel, I., Rico, R., Tsao, T.-C., and He, X. (2021). Somatosensory actuator based on stretchable conductive photothermally responsive hydrogel. Sci. Robot. *6*, eabd5483. https://doi.org/10.1126/scirobotics.abd5483.

74. Jiang, Z., Seraji, S.M., Tan, X., Zhang, X., Dinh, T., Mollazade, M., Rowan, A.E., Whittaker, A.K., Song, P., and Wang, H. (2021). Strong, Ultrafast, Reprogrammable Hydrogel Actuators with Muscle-Mimetic Aligned Fibrous Structures. Chem. Mater. *33*, 7818–7828. https://doi.org/10.1021/acs.chemmater.1c02312.

75. Mredha, M.T.I., Le, H.H., Tran, V.T., Trtik, P., Cui, J., and Jeon, I. (2019). Anisotropic tough multilayer hydrogels with programmable orientation. Mater. Horiz. *6*, 1504–1511. https://doi.org/10.1039/C9MH00320G.

76. Hua, M., Wu, S., Ma, Y., Zhao, Y., Chen, Z., Frenkel, I., Strzalka, J., Zhou, H., Zhu, X., and He, X. (2021). Strong tough hydrogels via the synergy of freeze-casting and salting out. Nature *590*, 594–599. https://doi.org/10.1038/s41586-021-03212-z.

77. Wu, J., Zhang, Z., Wu, Z., Liu, D., Yang, X., Wang, Y., Jia, X., Xu, X., Jiang, P., and Wang, X. Strong and Ultra-Tough Supramolecular Hydrogel Enabled by Strain-Induced Microphase Separation. Adv. Funct. Mater. n/a, 2210395. 10.1002/adfm.202210395.

78. Sun, D., Gao, Y., Zhou, Y., Yang, M., Hu, J., Lu, T., and Wang, T. (2022). Enhance Fracture Toughness and Fatigue Resistance of Hydrogels by Reversible Alignment of Nanofibers. ACS Appl. Mater. Interfaces *14*, 49389–49397. https://doi.org/10.1021/acsami.2c16273.

79. Choi, S., Moon, J.R., Park, N., Im, J., Kim, Y.E., Kim, J.-H., and Kim, J. Bone-Adhesive Anisotropic Tough Hydrogel Mimicking Tendon Enthesis. Adv. Mater. n/a, 2206207. 10.1002/adma.202206207.

80. He, J., Khalesi, H., Zhang, Y., Zhao, Y., and Fang, Y. (2022). Jerky-Inspired Fabrication of Anisotropic Hydrogels with Widely Tunable Mechanical Properties. Langmuir *38*, 10986–10993. https://doi.org/10.1021/acs.langmuir.2c01445.

81. Wei, P., Chen, T., Chen, G., Hou, K., and Zhu, M. (2021). Ligament-Inspired Tough and Anisotropic Fibrous Gel Belt with Programed Shape Deformations via Dynamic Stretching. ACS Appl. Mater. Interfaces *13*, 19291–19300. https://doi.org/10.1021/acsami.1c02351.

82. Li, G., Gao, T., Fan, G., Liu, Z., Liu, Z., Jiang, J., and Zhao, Y. (2020). Photoresponsive Shape Memory Hydrogels for Complex Deformation and Solvent-Driven Actuation. ACS Appl. Mater. Interfaces *12*, 6407–6418. https://doi.org/10.1021/acsami.9b19380.

83. Liang, X., Chen, G., Lin, S., Zhang, J., Wang, L., Zhang, P., Lan, Y., and Liu, J. (2022). Bioinspired 2D Isotropically Fatigue-Resistant Hydrogels. Adv. Mater. *34*, 2107106. https://doi.org/10.1002/adma.202107106.

84. Wang, X.-w., Wang, J., Yu, Y., Yu, L., Wang, Y.-x., Ren, K.-f., and Ji, J. (2022). A polyzwitterion-based antifouling and flexible bilayer hydrogel coating. Compos. B Eng. *244*, 110164. https://doi.org/10.1016/j.compositesb.2022.110164.

85. He, X., Wang, S., Zhou, J., Zhang, D., Xue, Y., Yang, X., Che, L., Li, D., Xiao, S., Liu, S., et al. (2022). Versatile and Simple Strategy for Preparing Bilayer Hydrogels with Janus Characteristics. ACS Appl. Mater. Interfaces *14*, 4579–4587. https://doi.org/10.1021/acsami.1c22887.

86. Liu, J., Miao, J., Zhao, L., Liu, Z., Leng, K., Xie, W., and Yu, Y. (2022). Versatile Bilayer Hydrogel for Wound Dressing through PET-RAFT Polymerization. Biomacromolecules *23*, 1112–1123. https://doi.org/10.1021/acs.biomac.1c01428.

87. Liu, S., Gao, G., Xiao, Y., and Fu, J. (2016). Tough and responsive oppositely charged nanocomposite hydrogels for use as bilayer actuators assembled through interfacial electrostatic attraction. J. Mater. Chem. B *4*, 3239–3246. https://doi.org/10.1039/C6TB00583G.

88. Ma, C., Li, T., Zhao, Q., Yang, X., Wu, J., Luo, Y., and Xie, T. (2014). Supramolecular Lego Assembly Towards Three-Dimensional Multi-Responsive Hydrogels. Adv. Mater. *26*, 5665–5669. https://doi.org/10.1002/adma.201402026.

89. Yao, C., Liu, Z., Yang, C., Wang, W., Ju, X.-J., Xie, R., and Chu, L.-Y. (2016). Smart Hydrogels with Inhomogeneous Structures Assembled Using Nanoclay-Cross-Linked Hydrogel Subunits as Building Blocks. ACS Appl. Mater. Interfaces *8*, 21721–21730. https://doi.org/10.1021/acsami.6b07713.

90. Chen, Z., Liu, J., Chen, Y., Zheng, X., Liu, H., and Li, H. (2021). Multiple-Stimuli-Responsive and Cellulose Conductive Ionic Hydrogel for Smart Wearable Devices and Thermal Actuators. ACS Appl. Mater. Interfaces *13*, 1353–1366. https://doi.org/10.1021/acsami.0c16719.

91. Ma, C., Lu, W., Yang, X., He, J., Le, X., Wang, L., Zhang, J., Serpe, M.J., Huang, Y., and Chen, T. (2018). Bioinspired Anisotropic Hydrogel Actuators with On–Off Switchable and Color-Tunable Fluorescence Behaviors.

Adv. Funct. Mater. *28*, 1704568. https://doi.org/10.1002/adfm.201704568.

92. Hubbard, A.M., Cui, W., Huang, Y., Takahashi, R., Dickey, M.D., Genzer, J., King, D.R., and Gong, J.P. (2019). Hydrogel/Elastomer Laminates Bonded via Fabric Interphases for Stimuli-Responsive. Matter *1*, 674–689. https://doi.org/10.1016/j.matt.2019.04.008.

93. Li, H., Liang, Y., Gao, G., Wei, S., Jian, Y., Le, X., Lu, W., Liu, Q., Zhang, J., and Chen, T. (2021). Asymmetric bilayer CNTs-elastomer/hydrogel composite as soft actuators with sensing performance. Chem. Eng. J. *415*, 128988. https://doi.org/10.1016/j.cej.2021.128988.

94. Zhu, Q.L., Dai, C.F., Wagner, D., Daab, M., Hong, W., Breu, J., Zheng, Q., and Wu, Z.L. (2020). Distributed Electric Field Induces Orientations of Nanosheets to Prepare Hydrogels with Elaborate Ordered Structures and Programmed Deformations. Adv. Mater. *32*, 2005567. https://doi.org/10.1002/adma.202005567.

95. Zhao, X., Kim, J., Cezar, C.A., Huebsch, N., Lee, K., Bouhadir, K., and Mooney, D.J. (2011). Active scaffolds for on-demand drug and cell delivery. Proc. Natl. Acad. Sci. USA *108*, 67–72. https://doi.org/10.1073/pnas.1007862108.

96. Ma, C., Le, X., Tang, X., He, J., Xiao, P., Zheng, J., Xiao, H., Lu, W., Zhang, J., Huang, Y., and Chen, T. (2016). A Multiresponsive Anisotropic Hydrogel with Macroscopic 3D Complex Deformations. Adv. Funct. Mater. *26*, 8670–8676. https://doi.org/10.1002/adfm.201603448.

97. Dong, M., Han, Y., Hao, X.P., Yu, H.C., Yin, J., Du, M., Zheng, Q., and Wu, Z.L. (2022). Digital Light Processing 3D Printing of Tough Supramolecular Hydrogels with Sophisticated Architectures as Impact-Absorption Elements. Adv. Mater. *34*, 2204333. https://doi.org/10.1002/adma.202204333.

98. Ma, Y., Hua, M., Wu, S., Du, Y., Pei, X., Zhu, X., Zhou, F., and He, X. (2020). Bioinspired high-power-density strong contractile hydrogel by programmable elastic recoil. Sci. Adv. *6*, eabd2520. https://doi.org/10.1126/sciadv.abd2520.

99. Liu, J., Xu, W., Kuang, Z., Dong, P., Yao, Y., Wu, H., Liu, A., and Ye, F. (2020). Gradient porous PNIPAM-based hydrogel actuators with rapid response and flexibly controllable deformation. J. Mater. Chem. C Mater. *8*, 12092–12099. https://doi.org/10.1039/D0TC00139B.

100. Park, N., and Kim, J. (2022). Anisotropic Hydrogels with a Multiscale Hierarchical Structure Exhibiting High Strength and Toughness for Mimicking Tendons. ACS Appl. Mater. Interfaces *14*, 4479–4489. https://doi.org/10.1021/acsami.1c18989.

101. Chen, G., Liang, X., Zhang, P., Lin, S., Cai, C., Yu, Z., and Liu, J. (2022). Bioinspired 3D Printing of Functional Materials by Harnessing Enzyme-Induced Biomineralization. Adv. Funct. Mater. *32*, 2113262. https://doi.org/10.1002/adfm.202113262.

102. Arslan, H., Nojoomi, A., Jeon, J., and Yum, K. (2019). 3D Printing of Anisotropic Hydrogels with Bioinspired Motion. Adv. Sci. *6*, 1800703. https://doi.org/10.1002/advs.201800703.

103. Takashima, Y., Hatanaka, S., Otsubo, M., Nakahata, M., Kakuta, T., Hashidzume, A., Yamaguchi, H., and Harada, A. (2012). Expansion–contraction of photoresponsive artificial muscle regulated by host–guest interactions. Nat. Commun. *3*, 1270. https://doi.org/10.1038/ncomms2280.

104. Hua, L., Zhao, C., Guan, X., Lu, J., and Zhang, J. (2022). Cold-induced shape memory hydrogels for strong and programmable artificial muscles. Sci. China Mater. *65*, 2274–2280. https://doi.org/10.1007/s40843-021-1971-9.

105. Keplinger, C., Sun, J.-Y., Foo, C.C., Rothemund, P., Whitesides, G.M., and Suo, Z. (2013). Stretchable, Transparent, Ionic Conductors. Science *341*, 984–987. https://doi.org/10.1126/science.1240228.

106. Li, T., Li, G., Liang, Y., Cheng, T., Dai, J., Yang, X., Liu, B., Zeng, Z., Huang, Z., Luo, Y., et al. (2017). Fast-moving soft electronic fish. Sci. Adv. *3*, e1602045. https://doi.org/10.1126/sciadv.1602045.

107. Wu, B., Jian, Y., Le, X., Lin, H., Wei, S., Lu, W., Zhang, J., Zhang, A., Huang, C.-F., and Chen, T. (2019). Supramolecular Fabrication of Complex 3D Hollow Polymeric Hydrogels with Shape and Function Diversity. ACS Appl. Mater. Interfaces *11*, 48564–48573. https://doi.org/10.1021/acsami.9b17440.

108. Yuk, H., Lin, S., Ma, C., Takaffoli, M., Fang, N.X., and Zhao, X. (2017). Hydraulic hydrogel actuators and robots optically and sonically camouflaged in water. Nat. Commun. *8*, 14230. https://doi.org/10.1038/ncomms14230.

109. Xu, W., Dong, P., Lin, S., Kuang, Z., Zhang, Z., Wang, S., Ye, F., Cheng, L., Wu, H., and Liu, A. (2022). Bioinspired bilayer hydrogel-based actuator with rapidly bidirectional actuation, programmable deformation and devisable functionality. Sensor. Actuator. B Chem. *359*, 131547. https://doi.org/10.1016/j.snb.2022.131547.

110. He, X., Zhu, J., and Yang, C. (2022). Harnessing osmotic swelling stress for robust hydrogel actuators. Soft Matter *18*, 5177–5184. https://doi.org/10.1039/D2SM00591C.

111. Li, Y., Liu, L., Xu, H., Cheng, Z., Yan, J., and Xie, X.-M. (2022). Biomimetic Gradient Hydrogel Actuators with Ultrafast Thermo-Responsiveness and High Strength. ACS Appl. Mater. Interfaces *14*, 32541–32550. https://doi.org/10.1021/acsami.2c07631.

112. Hong, W., Zhao, X., and Suo, Z. (2010). Large deformation and electrochemistry of polyelectrolyte gels. J. Mech. Phys. Solid. *58*, 558–577. https://doi.org/10.1016/j.jmps.2010.01.005.

113. Flory, P.J. (1945). Thermodynamics of dilute solutions of high polymers. J. Chem. Phys. *13*, 453–465.

114. Gierke, T.D., Munn, G.E., and Wilson, F.C. (1981). The morphology in nafion perfluorinated membrane products, as determined by wide- and small-angle x-ray studies. J. Polym. Sci. Polym. Phys. Ed *19*, 1687–1704. https://doi.org/10.1002/pol.1981.180191103.

115. Cai, S., and Suo, Z. (2012). Equations of state for ideal elastomeric gels. Europhys. Lett. *97*, 34009. https://doi.org/10.1209/0295-5075/97/34009.

116. Li, J., Hu, Y., Vlassak, J.J., and Suo, Z. (2012). Experimental determination of equations of state for ideal elastomeric gels. Soft Matter *8*, 8121–8128. https://doi.org/10.1039/C2SM25437A.

117. Fan, W., Shan, C., Guo, H., Sang, J., Wang, R., Zheng, R., Sui, K., and Nie, Z. (2019). Dual-gradient enabled ultrafast biomimetic snapping of hydrogel materials. Sci. Adv. *5*, eaav7174. https://doi.org/10.1126/sciadv.aav7174.

118. Alsaid, Y., Wu, S., Wu, D., Du, Y., Shi, L., Khodambashi, R., Rico, R., Hua, M., Yan, Y., Zhao, Y., et al. (2021). Tunable Sponge-Like Hierarchically Porous Hydrogels with Simultaneously Enhanced Diffusivity and Mechanical Properties. Adv. Mater. *33*, 2008235. https://doi.org/10.1002/adma.202008235.

119. Na, H., Kang, Y.-W., Park, C.S., Jung, S., Kim, H.-Y., and Sun, J.-Y. (2022). Hydrogel-based strong and fast actuators by electroosmotic turgor pressure. Science *376*, 301–307. https://doi.org/10.1126/science.abm7862.

120. Zheng, J., Xiao, P., Le, X., Lu, W., Théato, P., Ma, C., Du, B., Zhang, J., Huang, Y., and Chen, T. (2018). Mimosa inspired bilayer hydrogel actuator functioning in multi-environments. J. Mater. Chem. C Mater. *6*, 1320–1327. https://doi.org/10.1039/C7TC04879C.

121. Li, L., Zhang, Y., Lu, H., Wang, Y., Xu, J., Zhu, J., Zhang, C., and Liu, T. (2020). Cryopolymerization enables anisotropic polyaniline hybrid hydrogels with superelasticity and highly deformation-tolerant electrochemical energy storage. Nat. Commun. *11*, 62. https://doi.org/10.1038/s41467-019-13959-9.

122. Chen, L., Zhang, W., Dong, Y., Chen, Q., Ouyang, W., Li, X., Ying, X., and Huang, J. (2020). Polyaniline/Poly(acrylamide-co-sodium acrylate) Porous Conductive Hydrogels with High Stretchability by Freeze-Thaw-Shrink Treatment for Flexible Electrodes. Macromol. Mater. Eng. *305*, 1900737. https://doi.org/10.1002/mame.201900737.

123. Jiang, Z., Diggle, B., Shackleford, I.C.G., and Connal, L.A. (2019). Tough, Self-Healing Hydrogels Capable of Ultrafast Shape Changing. Adv. Mater. *31*, 1904956. https://doi.org/10.1002/adma.201904956.

124. Jian, Y., Wu, B., Yang, X., Peng, Y., Zhang, D., Yang, Y., Qiu, H., Lu, H., Zhang, J., and Chen, T. (2022). Stimuli-responsive hydrogel sponge for ultrafast responsive actuator. Supramolecular Materials *1*, 100002. https://doi.org/10.1016/j.supmat.2021.100002.

125. Osada, Y., Okuzaki, H., and Hori, H. (1992). A polymer gel with electrically driven motility. Nature *355*, 242–244. https://doi.org/10.1038/355242a0.

126. Wang, E., Desai, M.S., and Lee, S.-W. (2013). Light-Controlled Graphene-Elastin

Composite Hydrogel Actuators. Nano Lett. *13*, 2826–2830. https://doi.org/10.1021/nl401088b.

127. Lutz, G.J., and Rome, L.C. (1994). Built for Jumping: the Design of the Frog Muscular System. Science *263*, 370–372. https://doi.org/10.1126/science.8278808.

128. Astley, H.C., and Roberts, T.J. (2012). Evidence for a vertebrate catapult: elastic energy storage in the plantaris tendon during frog jumping. Biol. Lett. *8*, 386–389. https://doi.org/10.1098/rsbl.2011.0982.

129. Aeles, J., Lichtwark, G., Peeters, D., Delecluse, C., Jonkers, I., and Vanwanseele, B. (2018). Effect of a prehop on the muscle-tendon interaction during vertical jumps. J. Appl. Physiol. *124*, 1203–1211. https://doi.org/10.1152/japplphysiol.00462.2017.

130. Zhuo, J., Wu, B., Zhang, J., Peng, Y., Lu, H., Le, X., Wei, S., and Chen, T. (2022). Supramolecular Assembly of Shape Memory and Actuating Hydrogels for Programmable Shape Transformation. ACS Appl. Mater. Interfaces *14*, 3551–3558. https://doi.org/10.1021/acsami.1c21941.

131. Dayyoub, T., Maksimkin, A.V., Filippova, O.V., Tcherdyntsev, V.V., and Telyshev, D.V. (2022). Shape Memory Polymers as Smart Materials: A Review. Polymers *14*, 3511.

132. Wu, B., Lu, H., Le, X., Lu, W., Zhang, J., Théato, P., and Chen, T. (2021). Recent progress in the shape deformation of polymeric hydrogels from memory to actuation. Chem. Sci. *12*, 6472–6487. https://doi.org/10.1039/D0SC07106D.

133. Costa, D.C.S., Costa, P.D.C., Gomes, M.C., Chandrakar, A., Wieringa, P.A., Moroni, L., and Mano, J.F. (2022). Universal Strategy for Designing Shape Memory Hydrogels. ACS Mater. Lett. *4*, 701–706. https://doi.org/10.1021/acsmaterialslett.2c00107.

134. Lu, H., Wu, B., Yang, X., Zhang, J., Jian, Y., Yan, H., Zhang, D., Xue, Q., and Chen, T. (2020). Actuating Supramolecular Shape Memorized Hydrogel Toward Programmable Shape Deformation. Small *16*, 2005461. https://doi.org/10.1002/smll.202005461.

135. Kim, Y., Yuk, H., Zhao, R., Chester, S.A., and Zhao, X. (2018). Printing ferromagnetic domains for untethered fast-transforming soft materials. Nature *558*, 274–279. https://doi.org/10.1038/s41586-018-0185-0.

136. Deng, Y., Xi, J., Meng, L., Lou, Y., Seidi, F., Wu, W., and Xiao, H. (2022). Stimuli-Responsive nanocellulose Hydrogels: An overview. Eur. Polym. J. *180*, 111591. https://doi.org/10.1016/j.eurpolymj.2022.111591.

137. Wang, Z., Xu, Z., Zhu, B., Zhang, Y., Lin, J., Wu, Y., and Wu, D. (2022). Design, fabrication and application of magnetically actuated micro/nanorobots: a review. Nanotechnology *33*, 152001. https://doi.org/10.1088/1361-6528/ac43e6.

138. Kellaris, N., Gopaluni Venkata, V., Smith, G.M., Mitchell, S.K., and Keplinger, C. (2018). Peano-HASEL actuators: Muscle-mimetic, electrohydraulic transducers that linearly contract on activation. Sci. Robot. *3*, eaar3276. https://doi.org/10.1126/scirobotics.aar3276.

139. Yang, C., Wang, W., Yao, C., Xie, R., Ju, X.-J., Liu, Z., and Chu, L.-Y. (2015). Hydrogel Walkers with Electro-Driven Motility for Cargo Transport. Sci. Rep. *5*, 13622. https://doi.org/10.1038/srep13622.

140. Xavier, M.S., Tawk, C.D., Yong, Y.K., and Fleming, A.J. (2021). 3D-printed omnidirectional soft pneumatic actuators: Design, modeling and characterization. Sensor Actuator Phys. *332*, 113199. https://doi.org/10.1016/j.sna.2021.113199.

141. Chen, G., Yang, X., Zhang, X., and Hu, H. (2021). Water hydraulic soft actuators for underwater autonomous robotic systems. Appl. Ocean Res. *109*, 102551. https://doi.org/10.1016/j.apor.2021.102551.

142. Chen, Z., Chen, Y., Hedenqvist, M.S., Chen, C., Cai, C., Li, H., Liu, H., and Fu, J. (2021). Multifunctional conductive hydrogels and their applications as smart wearable devices. J. Mater. Chem. B *9*, 2561–2583. https://doi.org/10.1039/D0TB02929G.

143. Lin, X., Zhao, X., Xu, C., Wang, L., and Xia, Y. (2022). Progress in the mechanical enhancement of hydrogels: Fabrication strategies and underlying mechanisms. J. Polym. Sci. *60*, 2525–2542. https://doi.org/10.1002/pol.20220154.

144. Wirthl, D., Pichler, R., Drack, M., Kettlguber, G., Moser, R., Gerstmayr, R., Hartmann, F., Bradt, E., Kaltseis, R., Siket, C.M., et al. (2017). Instant tough bonding of hydrogels for soft machines and electronics. Sci. Adv. *3*, e1700053. https://doi.org/10.1126/sciadv.1700053.

145. Yu, R., Zhu, L., Xia, Y., Liu, J., Liang, J., Xu, J., Wang, B., and Wang, S. (2022). Octopus Inspired Hydrogel Actuator with Synergistic Structural Color and Shape Change. Adv. Mater. Interfac. *9*, 2200401. https://doi.org/10.1002/admi.202200401.

146. Ilievski, F., Mazzeo, A.D., Shepherd, R.F., Chen, X., and Whitesides, G.M. (2011). Soft Robotics for Chemists. Angew Chem. Int. Ed. Engl. *50*, 1890–1895. https://doi.org/10.1002/anie.201006464.

147. Mosadegh, B., Polygerinos, P., Keplinger, C., Wennstedt, S., Shepherd, R.F., Gupta, U., Shim, J., Bertoldi, K., Walsh, C.J., and Whitesides, G.M. (2014). Pneumatic Networks for Soft Robotics that Actuate Rapidly. Adv. Funct. Mater. *24*, 2163–2170. https://doi.org/10.1002/adfm.201303288.

148. Chathuranga, H., Marriam, I., Chen, S., Zhang, Z., MacLeod, J., Liu, Y., Yang, H., and Yan, C. (2022). Multistimulus-Responsive Graphene Oxide/Fe3O4/Starch Soft Actuators. ACS Appl. Mater. Interfaces *14*, 16772–16779. https://doi.org/10.1021/acsami.2c03486.

149. Zhu, Q.L., Du, C., Dai, Y., Daab, M., Matejdes, M., Breu, J., Hong, W., Zheng, Q., and Wu, Z.L. (2020). Light-steered locomotion of muscle-like hydrogel by self-coordinated shape change and friction modulation. Nat. Commun. *11*, 5166. https://doi.org/10.1038/s41467-020-18801-1.

150. Gao, G., Wang, Z., Xu, D., Wang, L., Xu, T., Zhang, H., Chen, J., and Fu, J. (2018). Snap-Buckling Motivated Controllable Jumping of Thermo-Responsive Hydrogel Bilayers. ACS Appl. Mater. Interfaces *10*, 41724–41731. https://doi.org/10.1021/acsami.8b16402.

151. Li, Z., Myung, N.V., and Yin, Y. (2021). Light-powered soft steam engines for self-adaptive oscillation and biomimetic swimming. Sci. Robot. *6*, eabi4523. https://doi.org/10.1126/scirobotics.abi4523.

152. Sun, Z., Song, C., Zhou, J., Hao, C., Liu, W., Liu, H., Wang, J., Huang, M., He, S., and Yang, M. (2021). Rapid Photothermal Responsive Conductive MXene Nanocomposite Hydrogels for Soft Manipulators and Sensitive Strain Sensors. Macromol. Rapid Commun. *42*, 2100499. https://doi.org/10.1002/marc.202100499.

153. Zhao, Q., Wang, Y., Cui, H., and Du, X. (2019). Bio-inspired sensing and actuating materials. J. Mater. Chem. C Mater. *7*, 6493–6511. https://doi.org/10.1039/C9TC01483G.

154. Morales, D., Palleau, E., Dickey, M.D., and Velev, O.D. (2014). Electro-actuated hydrogel walkers with dual responsive legs. Soft Matter *10*, 1337–1348. https://doi.org/10.1039/C3SM51921J.

155. Kim, Y., van den Berg, J., and Crosby, A.J. (2021). Autonomous snapping and jumping polymer gels. Nat. Mater. *20*, 1695–1701. https://doi.org/10.1038/s41563-020-00909-w.

156. Lee, H., Xia, C., and Fang, N.X. (2010). First jump of microgel; actuation speed enhancement by elastic instability. Soft Matter *6*, 4342–4345. https://doi.org/10.1039/C0SM00092B.

157. Zhang, X., Xue, P., Yang, X., Valenzuela, C., Chen, Y., Lv, P., Wang, Z., Wang, L., and Xu, X. (2022). Near-Infrared Light-Driven Shape-Programmable Hydrogel Actuators Loaded with Metal–Organic Frameworks. ACS Appl. Mater. Interfaces *14*, 11834–11841. https://doi.org/10.1021/acsami.1c24702.

158. Wang, Y., Xie, S., Bai, Y., Suo, Z., and Jia, K. (2021). Transduction between magnets and ions. Mater. Horiz. *8*, 1959–1965. https://doi.org/10.1039/D1MH00418B.

159. Jiang, G., Wang, G., Zhu, Y., Cheng, W., Cao, K., Xu, G., Zhao, D., and Yu, H. (2022). A Scalable Bacterial Cellulose Ionogel for Multisensory Electronic Skin. Research *2022*, 9814767. https://doi.org/10.34133/2022/9814767.

160. Pang, Y., Xu, X., Chen, S., Fang, Y., Shi, X., Deng, Y., Wang, Z.-L., and Cao, C. (2022). Skin-inspired textile-based tactile sensors enable multifunctional sensing of wearables and soft robots. Nano Energy *96*, 107137. https://doi.org/10.1016/j.nanoen.2022.107137.

161. Liu, H., Wei, S., Qiu, H., Si, M., Lin, G., Lei, Z., Lu, W., Zhou, L., and Chen, T. (2022). Supramolecular Hydrogel with Orthogonally Responsive R/G/B Fluorophores Enables Multi-Color Switchable Biomimetic Soft Skins. Adv. Funct. Mater. *32*, 2108830. https://doi.org/10.1002/adfm.202108830.

162. Wang, M., Zhang, P., Shamsi, M., Thelen, J.L., Qian, W., Truong, V.K., Ma, J., Hu, J., and Dickey, M.D. (2022). Tough and stretchable ionogels by in situ phase separation. Nat. Mater. *21*, 359–365. https://doi.org/10.1038/s41563-022-01195-4.

163. Zou, Q., Wang, Y., and Yang, F. (2021). An intrinsically embedded pressure-temperature dual-mode soft sensor towards soft robotics. Sensor Actuator Phys. *332*, 113084. https://doi.org/10.1016/j.sna.2021.113084.

164. Wei, S., Lu, W., Le, X., Ma, C., Lin, H., Wu, B., Zhang, J., Theato, P., and Chen, T. (2019). Bioinspired Synergistic Fluorescence-Color-Switchable Polymeric Hydrogel Actuators. Angew Chem. Int. Ed. Engl. *58*, 16243–16251. https://doi.org/10.1002/anie.201908437.

165. Li, K., Li, Z., Xiong, Z., Wang, Y., Yang, H., Xu, W., Jing, L., Ding, M., Zhu, J., Ho, J.S., and Chen, P.-Y. Thermal Camouflaging MXene Robotic Skin with Bio-Inspired Stimulus Sensation and Wireless Communication. Adv. Funct. Mater. n/a, 2110534. 10.1002/adfm.202110534.

166. Li, B., Kan, L., Li, C., Li, W., Zhang, Y., Li, R., Wei, H., Zhang, X., and Ma, N. (2021). Adaptable ionic liquid-containing supramolecular hydrogel with multiple sensations at subzero temperatures. J. Mater. Chem. C Mater. *9*, 1044–1050. https://doi.org/10.1039/D0TC04992A.

167. Baines, R., Patiballa, S.K., Booth, J., Ramirez, L., Sipple, T., Garcia, A., Fish, F., and Kramer-Bottiglio, R. (2022). Multi-environment robotic transitions through adaptive morphogenesis. Nature *610*, 283–289. https://doi.org/10.1038/s41586-022-05188-w.

168. Chen, Z., Lou, R., Zhong, D., Xiao, R., Qu, S., and Yang, W. (2021). An anisotropic constitutive model for 3D printed hydrogel-fiber composites. J. Mech. Phys. Solid. *156*, 104611. https://doi.org/10.1016/j.jmps.2021.104611.

169. Chen, Z., Zhao, D., Liu, B., Nian, G., Li, X., Yin, J., Qu, S., and Yang, W. (2019). 3D Printing of Multifunctional Hydrogels. Adv. Funct. Mater. *29*, 1900971. https://doi.org/10.1002/adfm.201900971.

170. Han, Z., Wang, P., Mao, G., Yin, T., Zhong, D., Yiming, B., Hu, X., Jia, Z., Nian, G., Qu, S., and Yang, W. (2020). Dual pH-Responsive Hydrogel Actuator for Lipophilic Drug Delivery. ACS Appl. Mater. Interfaces *12*, 12010–12017. https://doi.org/10.1021/acsami.9b21713.

171. Chen, R., Li, X., Xiong, Q., Zhu, X., Wang, H., Wang, W., Bao, G., Chen, Z., Chase Cao, C., and Luo, J. (2023). A Self-healable, recyclable and degradable soft network structure material for soft robotics. Mater. Des. *227*, 111783. https://doi.org/10.1016/j.matdes.2023.111783.

172. Liu, X., Song, M., Fang, Y., Zhao, Y., and Cao, C. (2022). Worm-Inspired Soft Robots Enable Adaptable Pipeline and Tunnel Inspection. Advanced Intelligent Systems *4*, 2100128. https://doi.org/10.1002/aisy.202100128.

173. Chen, J., Chen, J., Zhu, Z., Sun, T., Liu, M., Lu, L., Zhou, C., and Luo, B. (2022). Drug-Loaded and Anisotropic Wood-Derived Hydrogel Periosteum with Super Antibacterial, Anti-Inflammatory, and Osteogenic Activities. ACS Appl. Mater. Interfaces *14*, 50485–50498. https://doi.org/10.1021/acsami.2c12147.

174. Shen, K.-H., Lu, C.-H., Kuo, C.-Y., Li, B.-Y., and Yeh, Y.-C. (2021). Smart near infrared-responsive nanocomposite hydrogels for therapeutics and diagnostics. J. Mater. Chem. B *9*, 7100–7116. https://doi.org/10.1039/D1TB00980J.

175. Cai, C., Zhu, H., Chen, Y., Guo, Y., Yang, Z., Li, H., and Liu, H. (2022). Mechanoactive Nanocomposite Hydrogel to Accelerate Wound Repair in Movable Parts. ACS Nano *16*, 20044–20056. https://doi.org/10.1021/acsnano.2c07483.

176. Li, M., Dong, Y., Wang, M., Lu, X., Li, X., Yu, J., and Ding, B. (2023). Hydrogel/nanofibrous membrane composites with enhanced water retention, stretchability and self-healing capability for wound healing. Compos. B Eng. *257*, 110672. https://doi.org/10.1016/j.compositesb.2023.110672.